

STUDY OF METAL-CNT CONTACT FOR GAS SENSING

A DISSERTATION

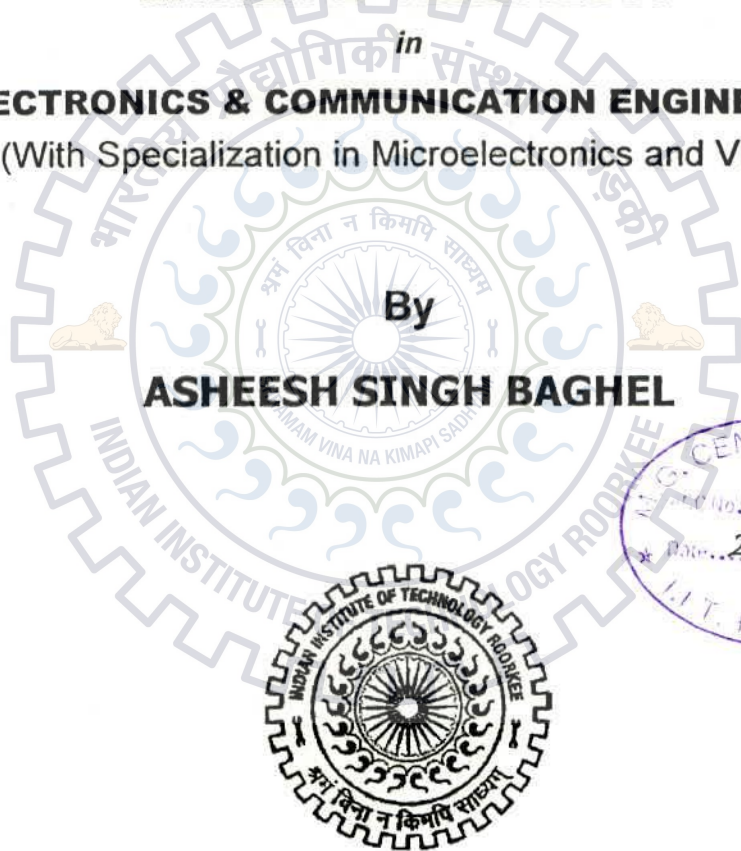
*Submitted in Partial fulfillment of the
requirements for the award of the degree
of*

MASTER OF TECHNOLOGY

in
ELECTRONICS & COMMUNICATION ENGINEERING
(With Specialization in Microelectronics and VLSI)

By

ASHEESH SINGH BAGHEL



DEPARTMENT OF ELECTRONICS AND COMMUNICATION ENGINEERING
INDIAN INSTITUTE OF TECHNOLOGY ROORKEE
ROORKEE -247 667 (INDIA)
JUNE, 2013


CANDIDATE'S DECLARATION

I hereby declare that the work, which is being reported in this dissertation entitled, "**Study of metal - CNT contact for gas sensing**", which is being submitted in the partial fulfilment of the requirements for the award of degree **Master of Technology in Microelectronics & VLSI**, submitted in the Department of Electronics and Communication Engineering, Indian Institute of Technology Roorkee, Roorkee (India), is an authentic record of my own work carried out from June 2012 to May 2013 under the guidance and supervision of **Dr. Ashok K. Saxena**, Professor and **Dr. Sanjeev Manhas**, Assistant Professor, Department of Electronics and Communication Engineering, Indian Institute of Technology Roorkee, Roorkee.

The results embodied in this report have not been submitted for the award of any other degree or diploma.

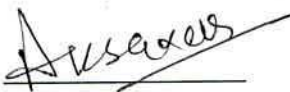
Dated: 27/06/12

Place: Roorkee


(Asheesh Singh Baghel)

CERTIFICATE

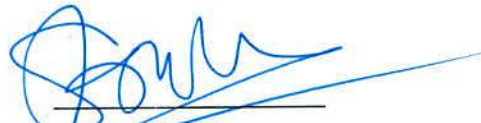
This is to certify that the above statement made by the candidate is correct to the best of my knowledge.



Dr. Ashok K. Saxena

Professor

Indian Institute of Technology, Roorkee



Dr. Sanjeev Manhas

Assistant Professor

Indian Institute of Technology, Roorkee

ABSTRACT

Two terminal CNT-Metal contact devices are fabricated using different metals (Nickel, Copper and Aluminum). I-V characteristics of fabricated devices are studied. The barrier height at the CNT-metal contacts is found for these metals using thermionic emission current. Nickel contacts shown the maximum conductance and least barrier height whereas Aluminum contacts shown least conductance and maximum barrier height among the chosen metals. Gases (Carbon Dioxide, Nitrogen and Methane) are used to investigate for gas sensing studies on these devices. The fabricated devices showed a high sensitivity for Carbon dioxide and methane altering the conductance of the devices substantially. They showed very small response time but very large recovery time. Nitrogen adsorbs weakly and thus does not affect the conductance of the devices as other gases.

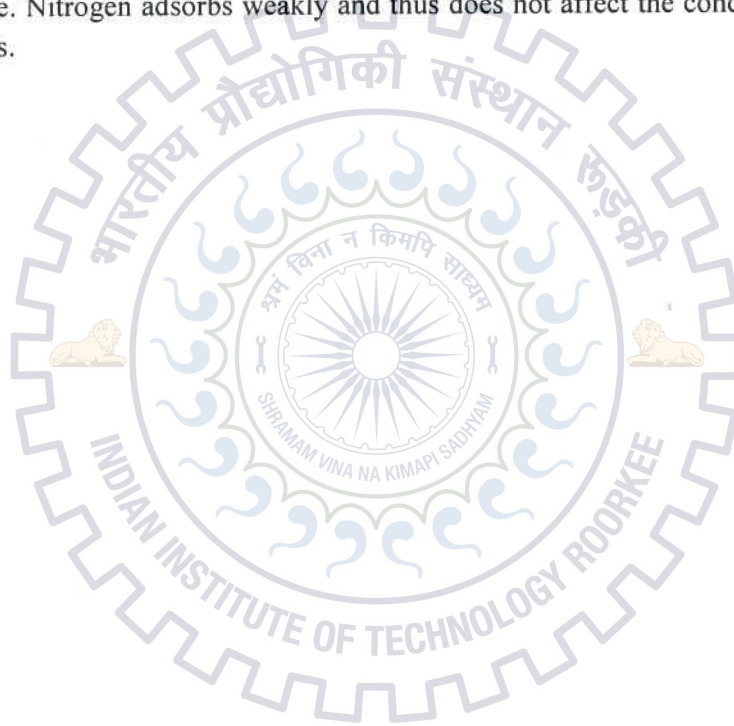
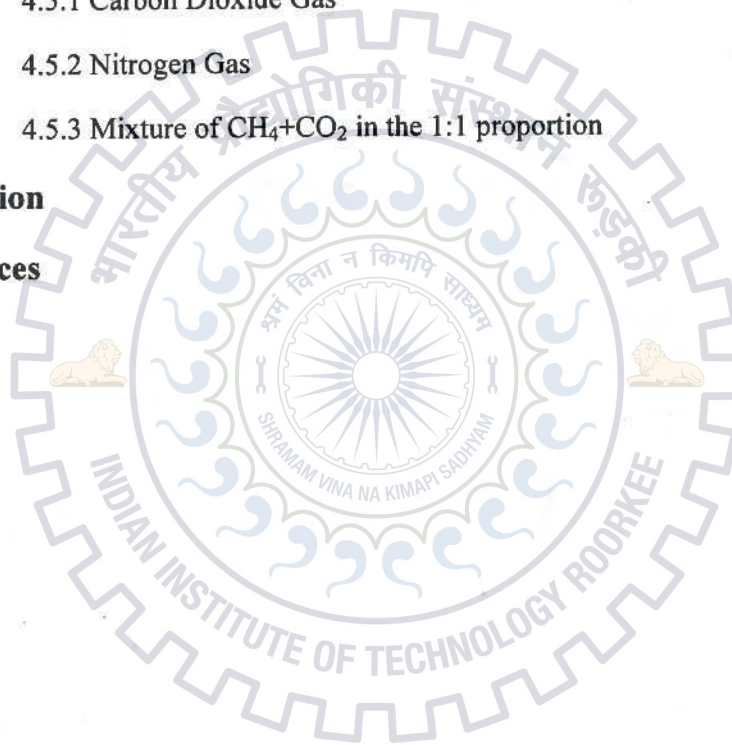


Table of Content

<i>Abstract</i>	<i>ii</i>
<i>Table of Content</i>	<i>iii</i>
<i>List of Figures</i>	<i>iv</i>
1. Introduction	1
1.1 Background & Motivation	3
2. Literature Survey	7
2.1 Carbon Nanotubes	7
2.2 High sensitivity of CNT	7
2.3 CNT-Metal Contacts	8
2.4 Fabrication of CNT based devices	10
2.5 CNT as chemical sensor	11
3. Fabrication & Characterization Setup	13
3.1 CNT used in the fabrication	13
3.2 Methods for forming channel using CNT	14
3.3 Process Flow chart	17
3.4 Characterization setup	18
4. Results & Analysis	20
4.1 FE-SEM images of CNT film & devices	20
4.2 Spectroscopy results	23
4.3 I-V characteristics of fabricated devices	25

4.1.1 Ni-CNT-Ni Device I-V Characteristics	26
4.1.2 Cu-CNT-Cu Device I-V Characteristics	26
4.1.3 Al-CNT-Al Device I-V Characteristics	27
4.1.4 Comparison of I-V of different metal-CNT contacts.	28
4.4 Thermionic Emission	29
4.2.1 Richardson's Law of Thermionic Emission	32
4.5 Effect of Gas on the Devices	35
4.5.1 Carbon Dioxide Gas	35
4.5.2 Nitrogen Gas	38
4.5.3 Mixture of $\text{CH}_4 + \text{CO}_2$ in the 1:1 proportion	40
5. Conclusion	43
6. References	44
Appendix	46



List of Figures

Fig1.1: Difference between forces acting on bulk and surface atoms	4
Fig 1.2 (a) Graphene Sheet, (b) CNT (Carbon Nanotubes)	5
Fig 2.1: Energy band diagram for metal- CNT before forming contact for the case $\phi_M > \phi_S$	8
Fig 2.2: Energy band diagram for metal- CNT contacts for the case $\phi_M > \phi_S$	9
Fig 2.3: Energy band diagram for metal- CNT before forming contact for the case $\phi_M < \phi_S$	9
Fig 2.4: Energy band diagram for metal- CNT contacts for the case $\phi_M < \phi_S$	9
Fig 2.5: Electrical conductance response of a semiconducting SWNT to (A) 200 ppm NO ₂ and (B) 1% NH ₃ vapor	11
Fig 3.1: A Simplified Diagram showing the device structure.	13
Fig 3.2: A) An Individual CNT in a cylindrical SDS micelle, B) A seven tube bundle of CNT coated by SDS micelle.	14
Fig 3.3: Ultra Sonicator	15
Fig 3.4(A): Before Centrifuge, (B) After Centrifuge.	15
Fig 3.5: Magnified image of device by optical microscope	16
Fig 3.6: FE-SEM used for taking images	18
Fig 3.7: Characterization Setup	19
Fig 4.1: FE-SEM image showing the CNTs after the Sonication at a magnification of 20,000x	20
Fig 4.2: FE-SEM image showing the CNTs after the Sonication at a magnification of 50,000x	21
Fig 4.3: FE-SEM image showing the CNTs after the Sonication at a magnification of 100,000x	21

Fig 4.4: FE-SEM image showing the channel region of a device at a magnification of 500x	22
Fig 4.5: FE-SEM image showing the channel region of a device at a magnification of 5000x	22
Fig 4.6: Spectrum of channel region before dispersing the solution	23
Fig 4.7: Spectrum of channel region after dispersing the solution	23
Fig 4.8: Spectrum of channel region of another device after dispersing the solution	24
Fig 4.9: Diagram representing the model of the fabricated structure	25
Fig 4.10: I-V Characteristics of Ni-CNT-Ni devices	26
Fig 4.11: I-V Characteristics of Cu-CNT-Cu devices	27
Fig 4.12: I-V Characteristics of Al-CNT-Al devices	28
Fig 4.13: Comparison of I-V Characteristics of three different metal-CNT devices	28
Fig 4.14: Thermionic current in Ni contact devices	29
Fig 4.15: Thermionic current in Cu contact devices	30
Fig 4.16: Thermionic current in Al contact devices	31
Fig 4.17: Comparison of thermionic current of Ni, Cu and Al devices	31
Fig 4.18: Logarithmic plot showing decrease in the current in the device with subsequent measurement	32
Fig 4.19: Energy band diagram showing CNT and the three metals	34
Fig 4.20: Plot Showing the Effect of Application of Carbon Dioxide gas on the device	36
Fig 4.21: Plot showing a 12 min sweep just after the application of Carbon Dioxide gas	37
Fig 4.22: Increase in temperature leads to desorption of the adsorbed gas	37
Fig 4.23: Plot Showing the Effect of Application of Carbon Dioxide gas on the device	38
Fig 4.24: Plot showing the effect of application of N ₂ gas on Al-CNT device	39
Fig 4.25: Plot showing the effect of application of N ₂ gas on Al-CNT device	39

Fig 4.26: Plot showing the effect of application of N_2 gas on AI-CNT device	40
Fig 4.27: Plot showing the effect of application of CH_4+CO_2 gas on AI-CNT device	41
Fig 4.28: Plot showing the after effect of application of CH_4+CO_2 gas on AI-CNT device	41
Fig 4.29: Plot showing the effect of application of very small amount of CH_4+CO_2 gas on AI-CNT device	42
Fig 4.30: Plot showing the effect of application of nitrogen after CH_4+CO_2 gas.	42



Chapter 1: Introduction

Gases are omnipresent and of the three states of matter their existence is least felt. The reasons are the properties of the gases which shrouds its existence so well that we had to develop specific devices which can detect their presence around us. These special devices which sense the presence of any specific gas or a mixture of gases are called Gas Sensors.

Every chemical compound has different physical and electrical properties which comes from the different elements forming the compound, their number & position in the structure, properties of the bonds joining the elements. All the aforementioned differences cause different chemical tendencies; Gas Sensors employ these different chemical interactions for the detection of the gas.

A few types of Gas Sensors are mentioned below, all these types employ specific properties of any gas for detection.

- Electrochemical Sensors
- Metal-Oxide Sensors
- Calorimetric type Sensors (Catalytic Bead Sensor)
- Acoustic type Gas Sensors
- Infrared point Sensor
- Infrared open path detector
- Nondispersive infrared Sensors
- Photoionization Sensor
- Piezoelectric Microcantilever
- Thermal Conductivity Detector
- Flame Ionization detector
- Microwave Chemistry Sensor

All these are few types which find general application in industries and other places. Most of these are defined by the physical process they use for detection but when someone tries to make a sensor for any particular gas, the chemical properties of that gas only are important. We can certainly find out that whether any of the above mentioned sensors which are only processes are

able to produce significant sensitivity but there may be other physical or chemical processes which exposes the presence of that particular gas with higher sensitivity, resolution and faster recovery.

These Characteristics i.e. Sensitivity, Resolution, Response time & Recovery Time are standard measuring yardsticks for any sensor. These are defined as follows:

- **Sensitivity:** It is defined as the change in the indicating/measuring quantity of the sensor for a unit change in the measured quantity. A good sensor should have high sensitivity, eg: If the column of mercury in thermometer rises by 1cm for 1°C rise in temperature, we say the sensitivity is 1cm/°C.
- **Resolution:** It is defined as the minimum change in the measured quantity that can be measured by the device, eg: If the minimum reading on the thermometer scale is 1mm and it require 0.1°C change in temperature for that much rise in mercury column, then the resolution of this thermometer would be 0.1°C.
- **Response Time:** It is defined as the time taken by our gas sensor after exposure to gas to produce 10% to 90% of steady state output value. For an ideal sensor the response time should be independent of the measured quantity.
- **Recovery Time:** It is defined as the time taken by our gas sensor to return back from 90% of steady state value to 10% of steady state value. This quantity decides how quickly, the sensor will be ready for next sensing.

A Gas Sensor might be used to measure the concentration of a particular gas in a mixture of gases or alone that might be a required product of an industrial process or might be a by-product which has to be disposed and must be monitored. So there can be various application some of which are mentioned below:

- To monitor the concentration & ingredients of pollutants that are disposed by an industry to check and modify the manufacturing process and process variations.
- To Avoid any Industrial Hazards from happening, where poisonous gases are used or stored. Because such kind of gas leakage can cause huge loss of human life as well as destruction of environment.
- In automobiles and airplane engines it can be used to determine the composition of effluent. It can help to determine the quality of fuel and maintenance requirements of engine.

Whatever may be the applications, a sensor needs to perform in an environment and the variations in the environment changes the output of a sensor; these variations may be change in temperature, moisture and other impurities in the mixture. Sensor must be designed in such a way that it must not be affected by changes in the ambient; this can also be controlled by using various type of filters to capture moisture or other impurities, if there is any sensitivity; the sensor can also be kept in temperature controlled environment to avoid those variations.

1.1 Background & Motivation

Adsorption is one of the basic properties shown by all the gases; adsorption is the process of accumulation of chemical process on the surface of a material rather than in the bulk, in contrast Absorption occurs in the bulk. Adsorption is completely a surface phenomena and the extent of adsorption of any molecular species depends upon the area available for adsorption. Adsorption occurs because the atoms in the bulk are in an environment where forces acting on it from any side are balanced by forces acting from other sides but the atoms at the surface are unbalanced because they don't have atoms on the other side as shown figure 1.1. These unbalanced forces at the surface are the sole reason for adsorption.

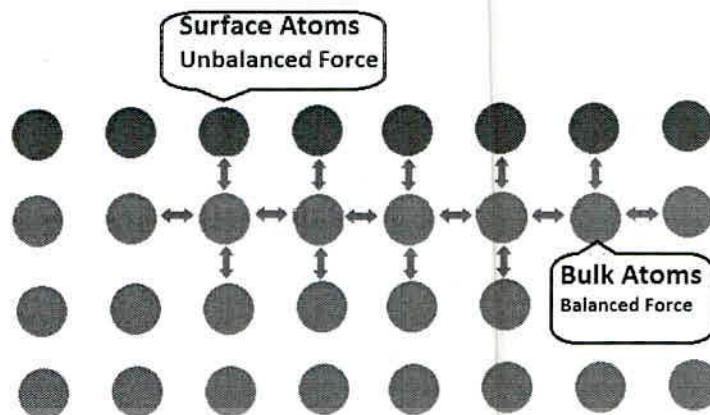


Fig1.1: Difference between forces acting on bulk and surface atoms.

The Adsorption can be divided into two different mechanisms: Physical Adsorption or Physisorption and Chemical Adsorption or Chemisorption. Van der Waal forces play the key role in Physisorption whereas actual chemical bond formation happens in Chemisorption. When the chemical species come near the surface, first van der waal forces attracts and retains the molecule at the surface leading to Physisorption, if we increase temperature now the energy of molecules increases leading to more vibration and the intermolecular forces holding them can't hold them enough and they get de-adsorbed, this process is called as desorption. The process of Physisorption is reversible but Chemisorption is not reversible as chemical bonds forms. Physisorption is exothermic process; when a chemical species get physically adsorbed on the adsorbate heat is released.



1.1

Now by using law of thermodynamics, if supply extra heat to this process, the equilibrium will shift to left side i.e. the adsorbed gas molecule will get desorbed, similarly if we decrease the pressure of the ambient, desorption of gas molecule will occur.

The process of Adsorption is highly dependent on the surface area of adsorbate; higher the surface area, more are the atoms which have unbalanced forces thus more adsorption can occur. Thus if we want to design a gas sensor, we need to use a material which has high surface to volume ratio. Porous materials, materials in finally divided state, nanomaterials have very high

surface to volume ratio and are thus suitable material for gas sensing applications but a material recently discovered also satisfy this criteria and that too with flying colors.

CNT (Carbon Nanotubes) can be described as sheets (graphene sheet) of carbon atoms (sp^2 hybridized, arranged in the shape of hexagons) rolled up in the form of cylinder.

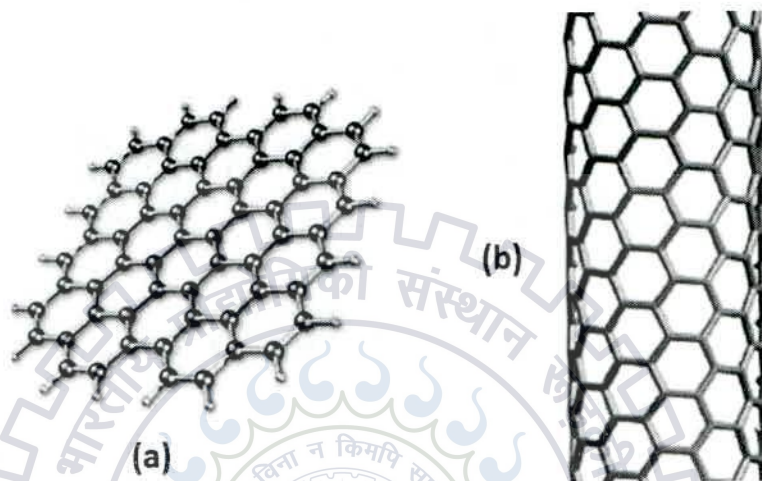


Fig 1.2 (a) Graphene Sheet, (b) CNT (Carbon Nanotubes).

Carbon Nanotubes has many fascinating properties but among them we are interested in very high electrical conductivity and very high surface to volume ratio. CNT can have only one cylinder (SWNT) or multiple cylinders stuffed inside each other like Russian doll (MWNT). All the carbon atoms of SWNT are at the surface, so all are possible site for adsorption, similarly in MWNT depending upon the gas only outer or inner layers may be available or not but nevertheless CNTs offer a surface to volume ratio not achievable from any material thus proves to be ideal candidate for adsorption based detectors.

Most of the existing sensors operate at elevated temperatures to achieve required reactivity and sensitivity. Carbon Nanotubes extremely high surface to volume ratio and presence of most of the atoms at the surface gives them capability to interact with most of the chemical species and the effect of those interactions changes the properties of the tube [13]. When a chemical entity interact with CNT, charge transfer takes place either from the CNT to that chemical entity leading to increase in hole concentration of tube or from the chemical entity to the tube leading to increase in the electron concentration at the tube [15], different molecules with entirely

different structures get adsorbed at different distances from the tube, different adsorption energy and charge transfer [15]. Except Charge transfer the adsorbed chemical species at the contact between tube and metal contact can modify the energy barrier at the contact by modifying the metal work function (eg: hydrogen gas modify the work function of finally divided platinum) [16]. The Schottky barrier at Metal-Nanotube junction severely limits the current in the otherwise ballistic nanotube [17].



2. Literature Survey

2.1 Carbon Nanotubes

After Iijima's identification of multi walled carbon nanotubes (MWCNTs) in 1991 [1], a huge interest in CNTs has been sparked by their extraordinary intrinsic properties. Because of their nanoscale dimensions, exceptionally high electrical and thermal conductivities, low density, high tensile strength and Young's modulus, MWCNTs have attracted considerable attention from both academic and technological areas to be an ideal material for sensing.

Three different kinds of CNTs are produced: single walled CNTs (SWCNTs), double walled CNTs (DWCNTs) and multi walled CNTs (MWCNTs). MWCNTs are the coaxial assembly of SWCNT cylinders rolled up with one another. Based on chirality and diameters, they are classified as armchair and zigzag. Chirality or twist of CNTs is the main characteristic that strongly determines electrical and other properties. According to the chirality, CNTs can be either metallic or semiconducting in nature. The exceptional electrical properties of CNTs are due to their one-dimensional character and uncommon electronic structure [2]. They possess extremely low electrical resistance. Electrical resistance is due to the collisions with defects in the crystal structure of a material when an electron flows. This defect can be a defect in the crystal structure, or vibration or impurity of an atom; electrons get deflected from their path because of such collisions and this scattering produces electrical resistance. But peculiarly, electrons in CNTs are not easily scattered due to their small diameter and very high length to diameter (aspect) ratio. Another peculiarity is that electrons in CNTs can move only forward and backward (1-D character). Only backscattering (moving forward and backward) can generate electrical resistance in CNTs. Backscattering occurs under the circumstances of strong collisions and it is very less likely to happen in case of CNTs. Thus due to very small possibilities of scattering, electrons in CNTs have extremely low electrical resistance. CNTs can be produced by many techniques of which (i) Chemical Vapor Deposition (CVD), (ii) Arc discharge and (iii) Laser Ablation methods are very common.

2.2 High Sensitivity of CNT

Due to the distortion of the electron clouds of CNTs from a uniform distribution in graphite to asymmetric distribution around cylindrical nanotubes, a rich π -electron conjugation forms outside of the CNTs, making them electrochemically active [3]. The electrical properties of

CNTs are extremely sensitive to charge transfer and chemical doping effects by various molecules. When electron-withdrawing molecules (e.g. NO_2 , O_2) or electron-donating molecules (e.g. NH_3) interact with the p-type semiconducting CNTs, they will change the density of the main charge carriers (i.e. holes) in the 'bulk' of the nanotube, which changes the conductance of CNTs. This behavior forms the basis for applications of CNTs as electrical chemical gas sensors. However, gas sensors based on pristine CNTs have certain limitations, such as sometimes low sensitivity to analyte for which they have low adsorption energy or low affinity, lack of selectivity, or irreversibility or long recovery time.

2.3 CNT-Metal Contacts

The contacts formed by semiconducting nanotubes are mostly Schottky contacts though the height of the barrier varies in accordance with the diameter and chirality of the nanotube as well as the work function of the metal. Process conditions and ambient condition role in deciding the barrier height has yet not been understood [15]. The presence of Schottky barrier greatly reduces the conductance of such contacts, way below the value of their quantum conductance which is $4e^2/h$ i.e. $1.54E-4$ Siemens [16].

Depending upon the band structure and position of Fermi level in relation to position of Fermi level there could be two types of barriers are possible which are shown below.

CASE I: $\phi_M > \phi_S$

Figure 2.1 represents the relative positions of Fermi level of semiconductor and Fermi level of metal for this case. Figure 2.2 represents the band structure at the junction of these two materials.

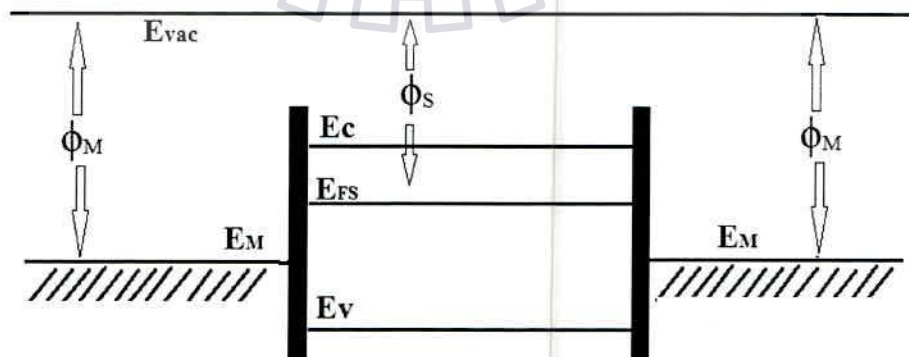


Fig 2.1: Energy band diagram for metal- CNT before forming contact for the case $\phi_M > \phi_S$.

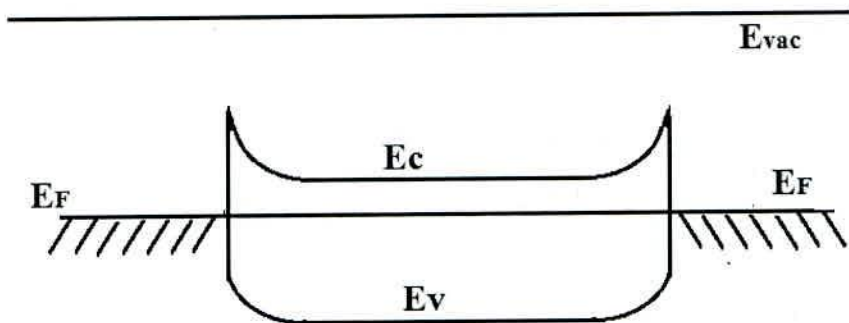


Fig 2.2: Energy band diagram for metal- CNT contacts for the case $\phi_M > \phi_S$.

CASE II: $\phi_M < \phi_S$

Figure 2.3 represents the relative positions of Fermi level of semiconductor and Fermi level of metal for this case. Figure 2.4 represents the band structure at the junction of these two materials.

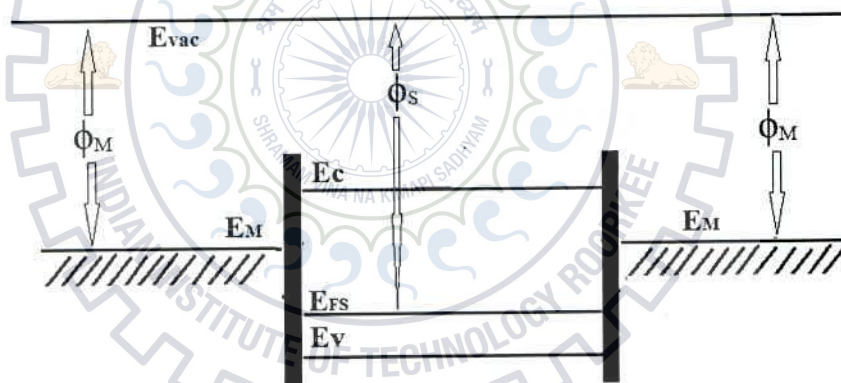


Fig 2.3: Energy band diagram for metal- CNT before forming contact for the case $\phi_M < \phi_S$

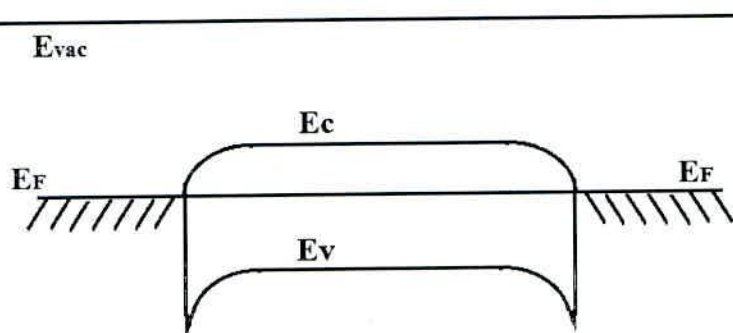


Fig 2.4: Energy band diagram for metal- CNT contacts for the case $\phi_M < \phi_S$

2.4 Fabrication of CNT based devices

Currently, there are mainly two methods to position CNTs across electrodes. One is to directly grow CNTs on the sensor platform via controlled chemical vapor deposition (CVD). The other is to drop-cast a CNT suspension or solution in water or in an organic solvent on top of prefabricated electrodes. The latter is sometimes followed by alignment or post-processing of the CNTs. The growth of CNTs on the sensor platform with CVD methods involves heating catalytic metal nanoparticles to high temperatures (500–1000 °C) in a furnace, and feeding a hydrocarbon gas (e.g. ethylene, acetylene or methane) for a period of time [4]. Iron, cobalt or nickel nanoparticles are often used as the catalysts. They are usually patterned on a support platform such as a silicon substrate with silicon dioxide as the insulating layer, or on a porous aluminum oxide substrate [4]. For MWNT growth, the growth temperature range is typically 550–750 °C, while the temperature required to form SWNTs is the range of 850–1000 °C. To form the electrode contacts with the CNTs, electrodes can be fabricated either by sputtering, evaporating or photo-lithographically patterning metal contacts such as gold pads over a single CNT or over a CNT network. CNTs can also be grown via CVD across prefabricated electrodes. In both cases, fabrication methods are complex and the yields are low. Inexpensive, high yield and reproducible fabrication techniques are essential for the success of CNT-based sensors.

Recent advances in carbon nanotube chemistry enable both the dissolution and dispersion of CNTs in various solvents [5]. These provide new alternative routes for fabricating CNT patterns by simply dispensing/printing the dissolved/dispersed particles on substrates. The sensor electrical resistance, which is dependent on the density of CNTs across the electrode contacts, can simply be tuned by adjusting the concentration of the CNTs in the dispersion or by adjusting the dispensed volume, in addition to drop casting of CNTs using micro-syringes, screen printing, inkjet printing and air brushing have been used sometimes followed by dielectrophoresis (DEP) to align the CNTs across the electrodes. Compared to the CVD-grown single SWNT-based sensor, these methods are more reproducible, cost effective and have higher yields.

Since CNTs conduct along their length, alignment is a factor that needs to be considered in improving directional anisotropic electrical properties. Due to their small sizes, it is extremely difficult to align nanotubes; lack of control of their orientation reduces the effectiveness of nanotube for structural or functional performance. During processing, application of magnetic

field, AC and DC electric field, spinning the melt in expected direction are some possible ways to improve the nanotube alignment.

2.5 CNT as chemical sensor

In 2000, Dai and coworkers first demonstrated that single semiconducting SWNTs can act as fast and sensitive Chem-FETs at ambient temperatures [8]. They fabricated individual semiconducting SWNT ChemFETs by growing SWNTs via CVD on SiO₂/Si substrates, then photo-lithographically patterning Ti/Au pads over a single SWNT for electrical contact (i.e. source and drain). The metal/semiconducting SWNT/metal system exhibited p-type transistor characteristics with several orders of magnitude change in conductance under various gate voltages. Upon exposure to NO₂ and NH₃, the conductance of the semiconducting SWNT changed dramatically. An increase in the conductance by three orders of magnitude was observed within several seconds when exposed to 200 ppm NO₂ ($V_g = +4$ V), while the conductance decreased about two orders of magnitude within two minutes when exposed to 10,000 ppm NH₃. Figure 2.1 demonstrates this fact.

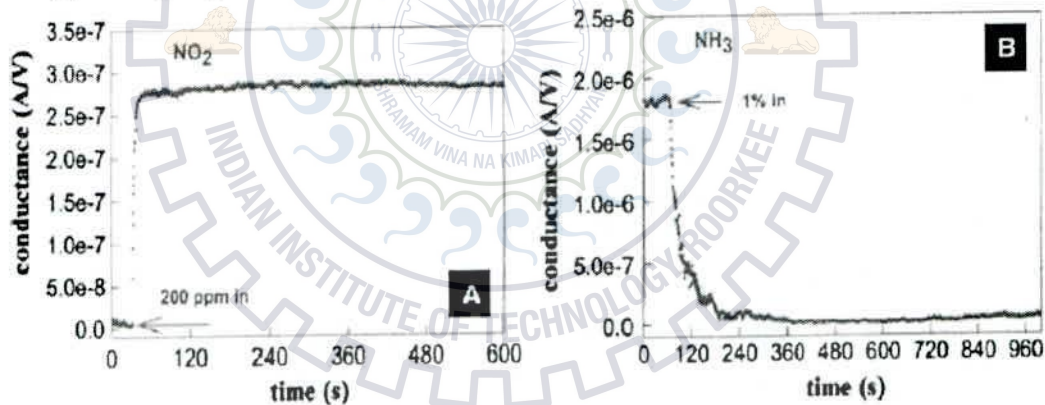
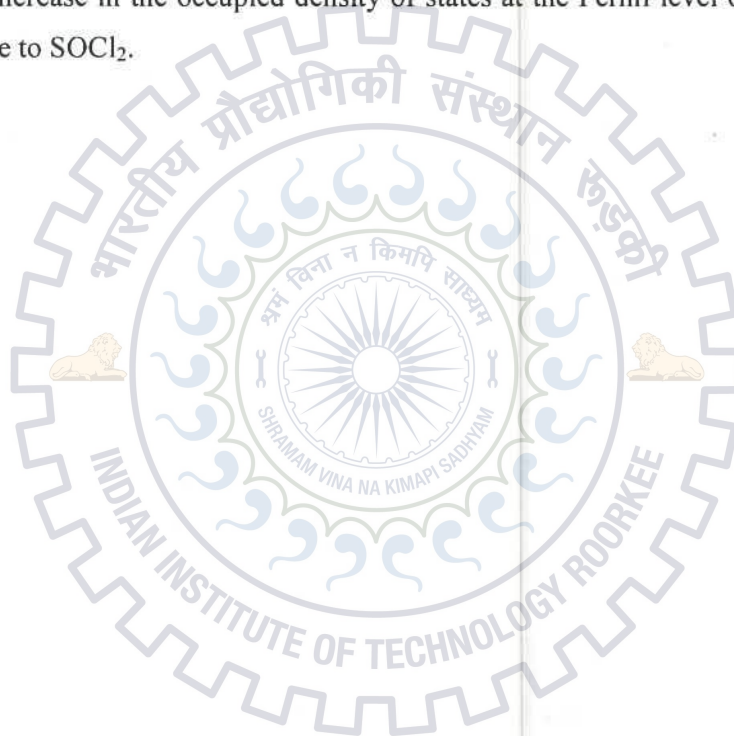


Fig 2.5: Electrical conductance response of a semiconducting SWNT to (A) 200 ppm NO₂ and (B) 1% NH₃ vapor

Suehiro *et al* fabricated an ammonia sensor based on MWNT networks using dielectrophoresis (DEP) [9]. DEP is the electro-kinetic motion of dielectrically polarized materials in non-uniform electric fields. The advantage of the DEP method is that the number of CNTs trapped in the region of interest can be controlled by the DEP force (e.g. frequency, amplitude) and by the duration of DEP trapping. MWNTs dispersed in ethanol were trapped and enriched in an interdigitated microelectrode gap using DEP. The authors investigated the changes in impedance in

response to exposure to 10 ppm NH₃. Measurements were conducted at a frequency of 100 kHz and 8 V AC bias at room temperature. The sensor conductance decreased dramatically, while the capacitance increased in the presence of ammonia. Lee *et al* fabricated metallic SWNT-based sensors using dielectrophoresis alignment after drop-casting of a suspension of SWNTs [10]. The sensors exhibited an increase in the conductance when exposed to thionyl chloride (SOCl₂, a nerve agent precursor) and dimethyl methylphosphonate (DMMP, a nerve agent stimulant), but the response was irreversible. They claimed that the signal transduction was mainly through the larger-diameter metallic nanotubes. The mechanism was proven by selective Raman decay showing an increase in the occupied density of states at the Fermi level of the metallic SWNTs after exposure to SOCl₂.



3. Fabrication & Characterization Setup

The basic requirement is to fabricate a two terminal device with Carbon Nanotubes (CNT) forming the channel between the two electrodes, so that changes in electrical characteristics of CNT with different gas molecules can be studied. CNTs have high electrical conductivity so the very large part of the net resistance offered by device will come from the contacts. In the case of sensors it's not required to form ohmic or near ohmic contacts. Following figure shows the basic idea of the device that we are trying to fabricate.

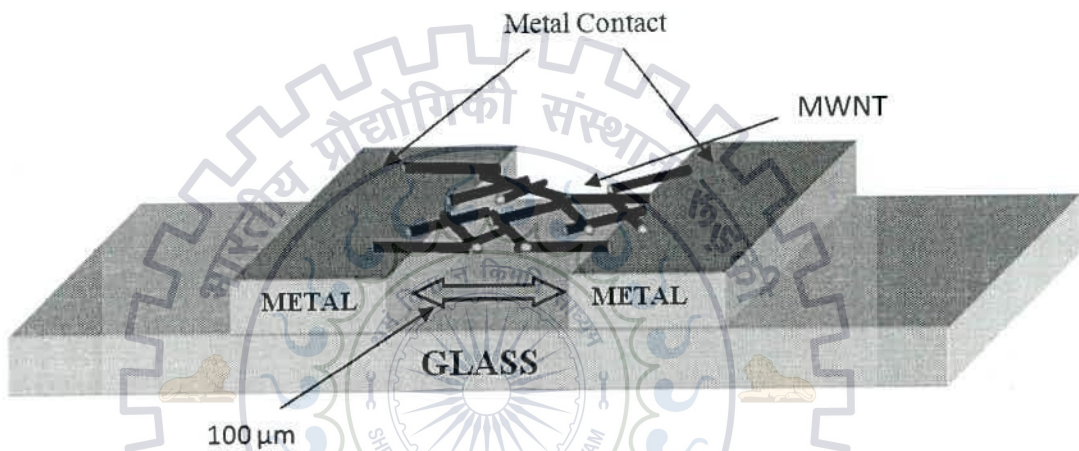


Fig 3.1: A Simplified Diagram showing the device structure.

3.1 CNT Used in the Fabrication

Carbon Nanotubes used in this process are Multiwalled Nanotubes (MWNT) in the form of powder; the powder has the purity of 95%, it contains some residual impurities from the fabrication process even after purification coming from the catalysts used, in the form of nickel, cobalt & iron etc. The tubes length vary from 0.5 μm to 200 μm ; the inside diameter varies from 5 to 10 nm and outside diameter varies from 10 to 20 nm. Complete technical specifications of the MWNT used as provided by the manufacturer are given in appendix A.

The MWNTs in the powder are of different chirality, so some would be zigzag and other would be of armchair structure with different diameters of inner and outer shells, in addition under the given circumstances some tubes would be of semiconducting type and other would be of metallic type. So we can say that we have a mixture of different tubes of unknown proportion.

3.2 Method for forming the channel using CNT

The Important Issues when handling the CNTs are:

- CNTs have very strong Van-der Waals interactions in the order of 500 eV [21].
- Aligning the CNTs lengthwise between the electrodes is a low efficiency process [22].
- There are residual impurities left after the fabrication, which generally are residues of catalyst used in the fabrication [22].

We decided to deposit the CNTs in between the electrode by making a suspension of CNTs in DI water and dispensing the solution over the electrode pattern by addressing the above mentioned issues.

Step 1: We used Sodium Dodecyl Sulfate (SDS) as the surfactant [17, 18, 21] to hold the tubes separated once they are untangled by sonication. SDS is an anionic surfactant and has a hydrophilic end and a hydrophobic end, the hydrophobic end attaches to the organic surface which is CNT here, they cluster around the bundles as shown in figure 2.2. If we manage to break these bundles, it will hold these separated tubes and will not allow them to form bundle again.

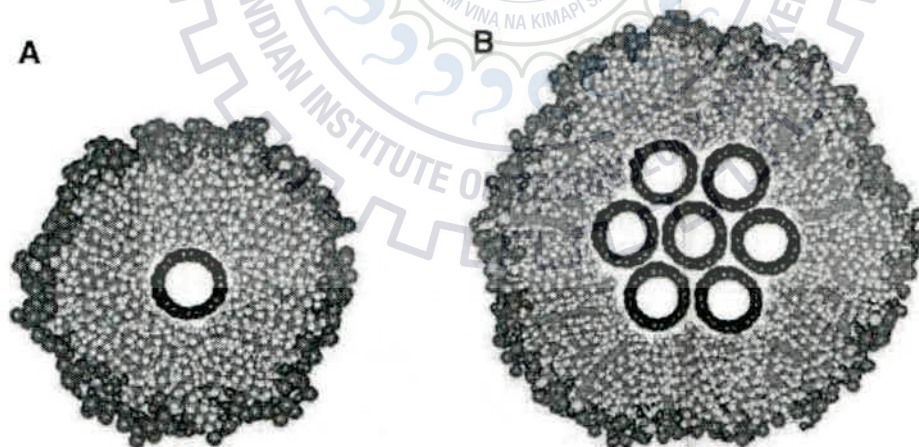


Fig 3.2: A) An Individual CNT in a cylindrical SDS micelle, B) A seven tube bundle of CNT coated by SDS micelle [18].

Step 2: Breaking the bundles: For breaking the CNT bundles we used Ultra-sonication at 540W for 10 minutes while maintaining the temperature at 25 degree Celsius using ice baths. The sonic waves at these high power breaks the bundles attached by strong van-der Waal forces and surfactant hold them separated [17].

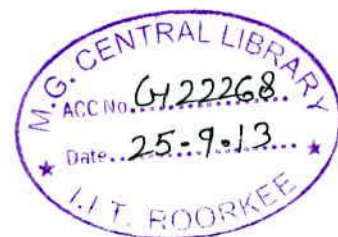


Fig 3.3: Ultra Sonicator.

Step 3: Removing Impurities: For removing the impurities and further breaking the bundles we used Centrifuge and operated it at the relative centrifugal force (RCF) of 26,000g for 6 hours. This removed the heavy Ni-Co catalyst impurities and CNTs which have very less density come at the top of the suspension. Carefully decant top 70% of the solution without disturbing the deposited supernatant at bottom. Figure 2.4 (A) shows the suspension before centrifuge, after sonication and Figure 2.4 (B) shows the suspension after the centrifuge [17, 18].

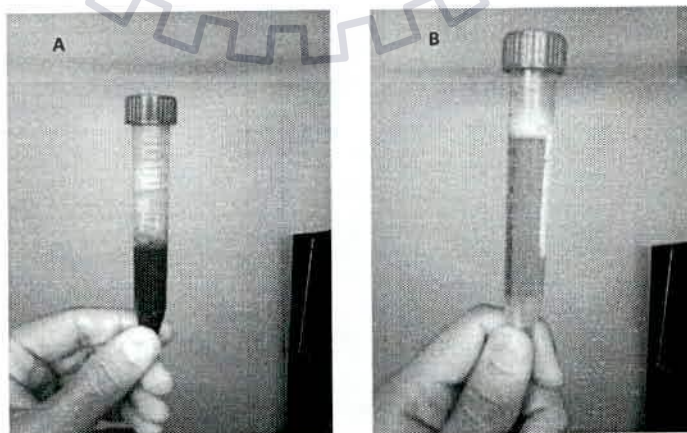


Fig 3.4(A): Before Centrifuge, (B) After Centrifuge.

Step 4: Aligning the CNTs: There are very few methods by which alignment of CNT can be done efficiently. Zhang & Iijima [23] tried by flowing Argon gas in the laser ablation reactor. Manipulating the CNTs using AFM tip [24] is destructive and low efficiency process. Yamanato, Akita and Nakayama demonstrated a simple and efficient method of aligning the tubes using electric field [25]. An induced dipole is developed on CNT when it is kept in an electric field. By applying different types of electric fields particle suspended in a solution can be moved because of a dipole induced by the applied field. For this we put a small drop of the solution in the channel between the patterned electrodes, apply 10MHz, 10 V_{p-p} sinusoidal using a function generator for 10 minutes [19, 20].

Step 5: Put the device in the oven for 2 minutes at 100 degree Celsius, this will evaporate the water. Let the device cool and come to room temperature before doing the characterization. Figure 2.5 shows an image of the finished device [17].

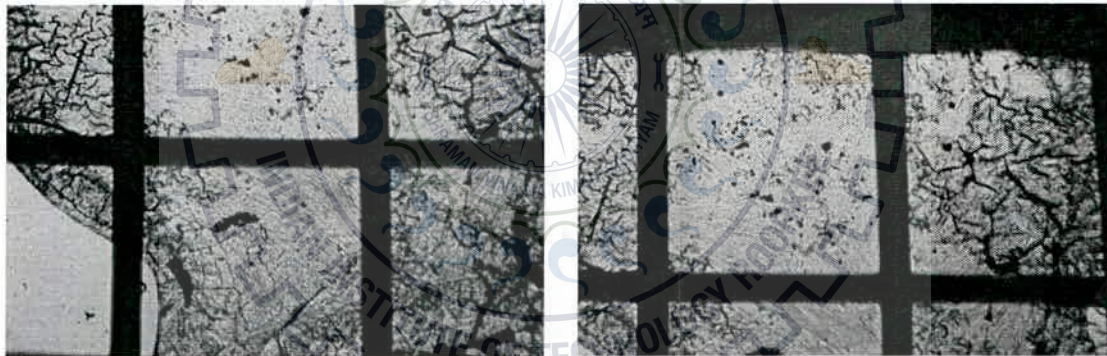
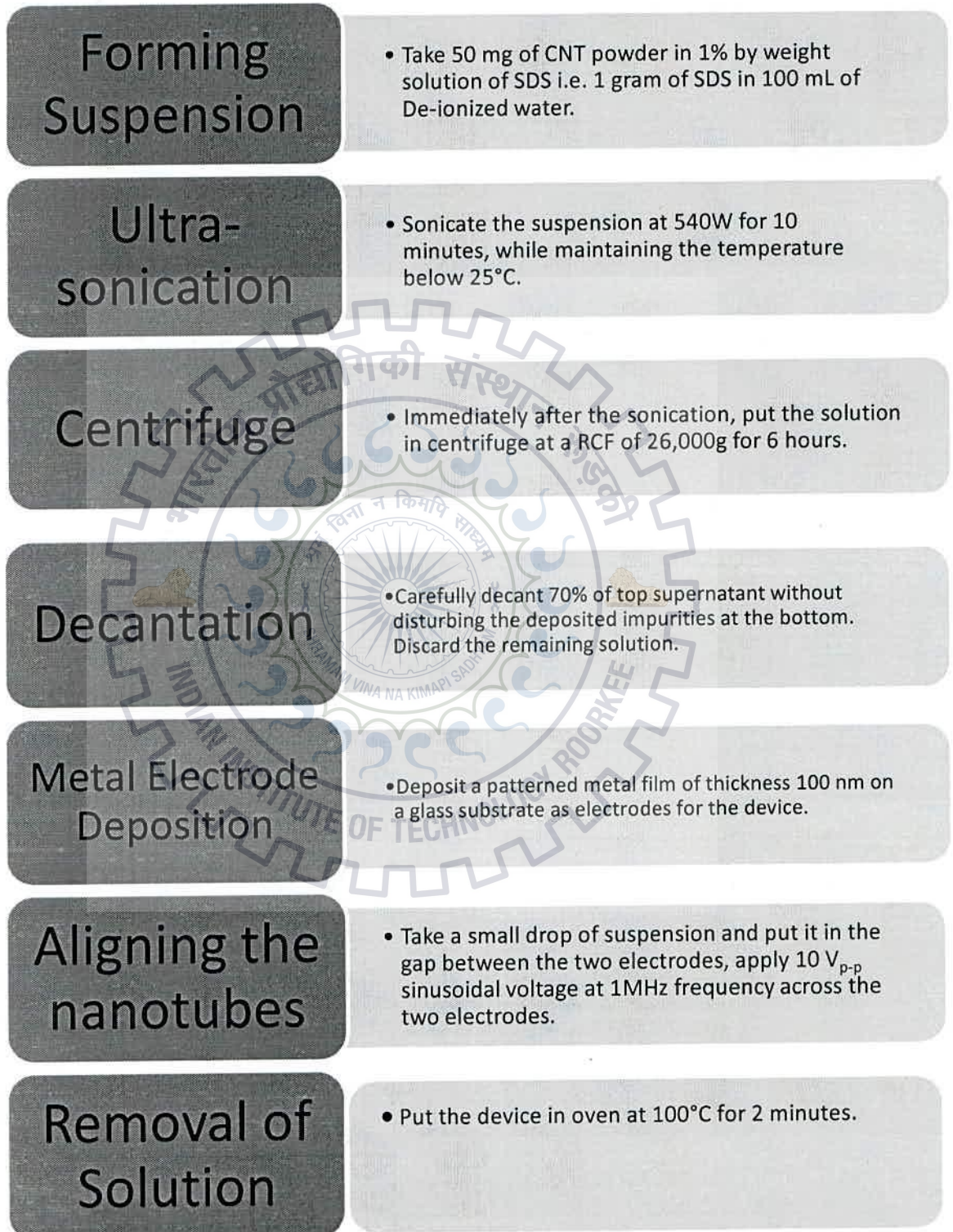


Fig 3.5: Magnified image of device by optical microscope at 5X, showing aluminum electrodes (bright squares), gap between the channel (dark stripes) having CNT dispersed, the peeling of aluminum electrode as seen in the figure is due to SDS.

2.3 Process Flow Chart



2.4 Characterization Setup

2.4.1 Structural Characterization

FE-SEM (Field Emission- Scanning Electron Microscope) is used to take the images of the suspension before and after centrifuge, images of nanotubes before and after aligning. For taking the SEM first the samples are sputtered with gold ions and then kept in SEM.

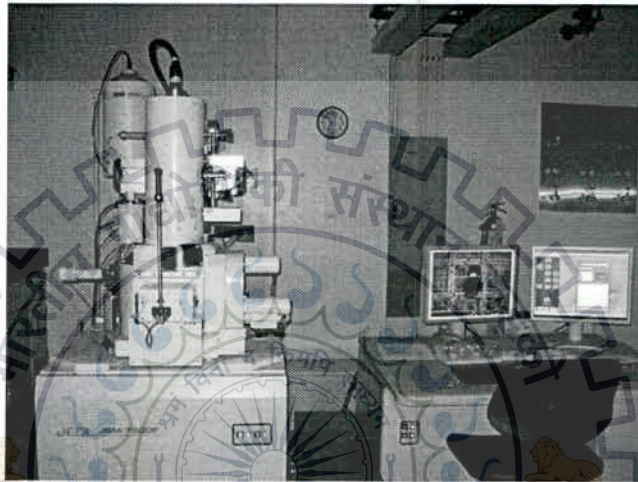


Fig 3.6: FE-SEM

Spectroscopy of channel before deposition and after deposition is done by the electron microscope which has the functionality of measuring the spectrum of any particular region.

We used the setup as shown in the figure 2.6 for electrical characterization and gas sensing studies; we did following type of measurements:

- I-V measurement using LabTracer software
- Biasing the device at a given fixed voltage for a given fixed time and obtaining the current passing through the device using a LabVIEW program driving the SMU for measuring the changes in current with respect to temperature and also measuring changes in current on application of gas.

Chuck is heated through a variac and the temperature is monitored using a thermocouple.

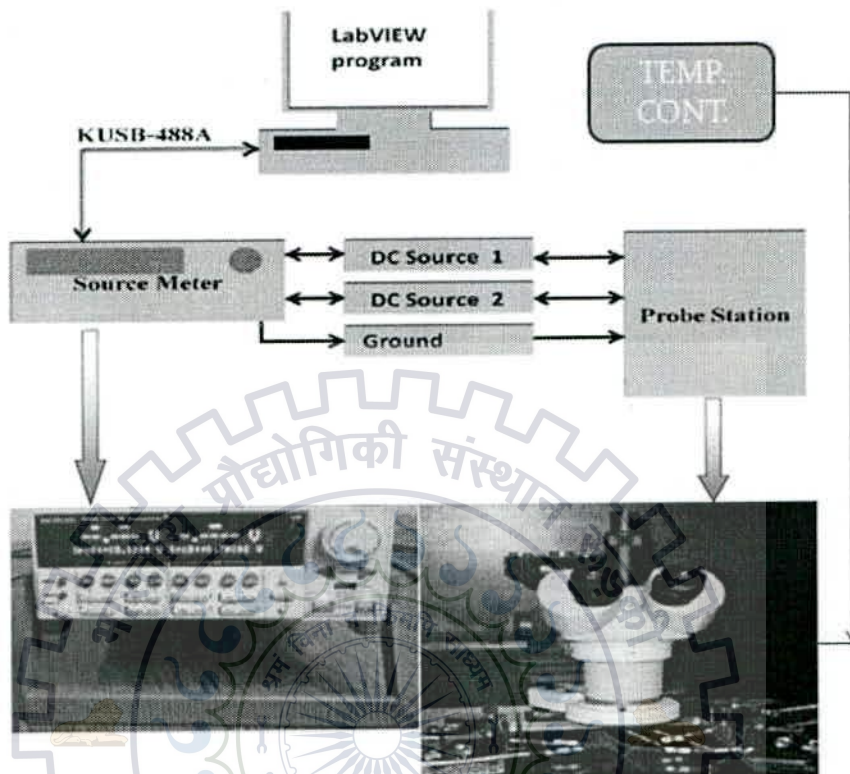


Fig 3.7: Electrical characterization Setup.

4. Results & Analysis

4.1 FE-SEM images of CNT film and devices.

Figure 4.1 shows a film of CNT suspension after sonication at a magnification of 20,000x, a very high density of CNT bundles can be seen. Figure 4.2 shows same film at 50,000x and figure 4.3 shows it at 100,000x. From these figures following points are evident:

- The CNTs are 1 μ m long on an average in contrast to the claim by manufacturer that it would be from 0.5 μ m to 200 μ m.
- The high degree of entanglement suggests that sonication has not been successful in separating the bundles.
- Alignment by electric field will have no impact in this high entangled system, for alignment to work, CNTs has to be separated by sonication.

Figure 4.4 and figure 4.5 are the images of the channel where the solution after centrifuge has been dispersed. No nanotubes are seen at the channel, instead a heap of flocculated particles appear at the channel. This flocculation may be because of impurities or because of heat provided during annealing of the contacts.

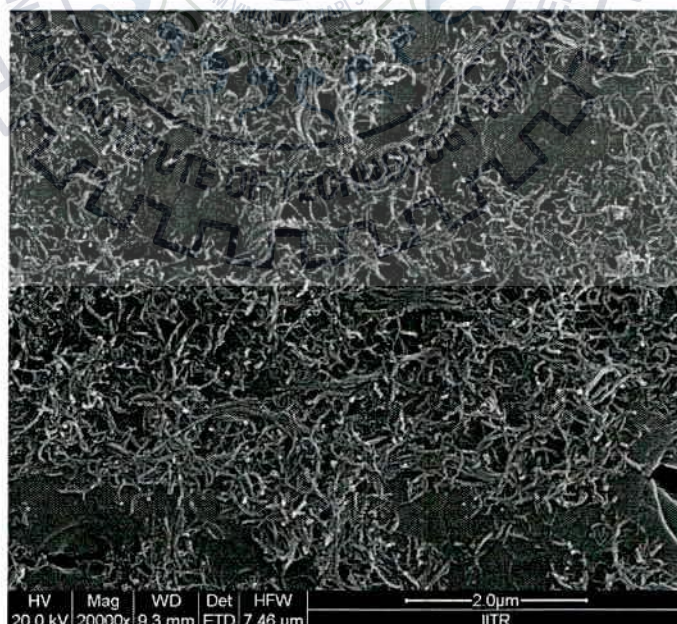


Fig 4.1: FE-SEM image showing the CNTs after the Sonication at a magnification of 20,000x.

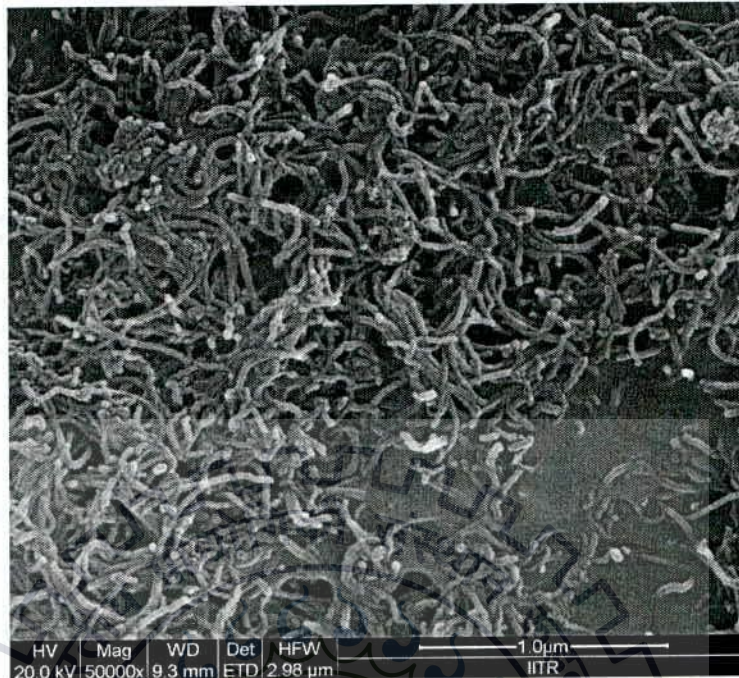


Fig 4.2: FE-SEM image showing the CNTs after the Sonication at a magnification of 50,000x.

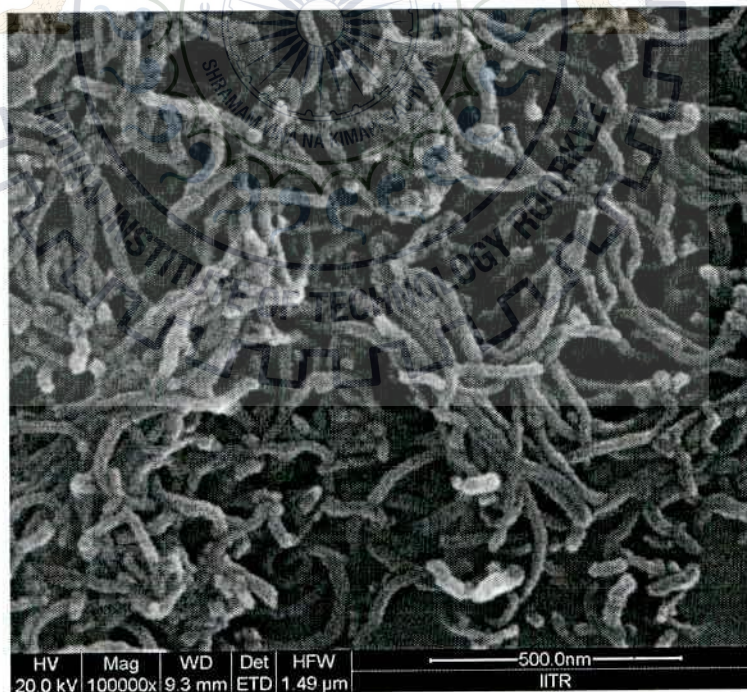


Fig 4.3: FE-SEM image showing the CNTs after the Sonication at a magnification of 100,000x.

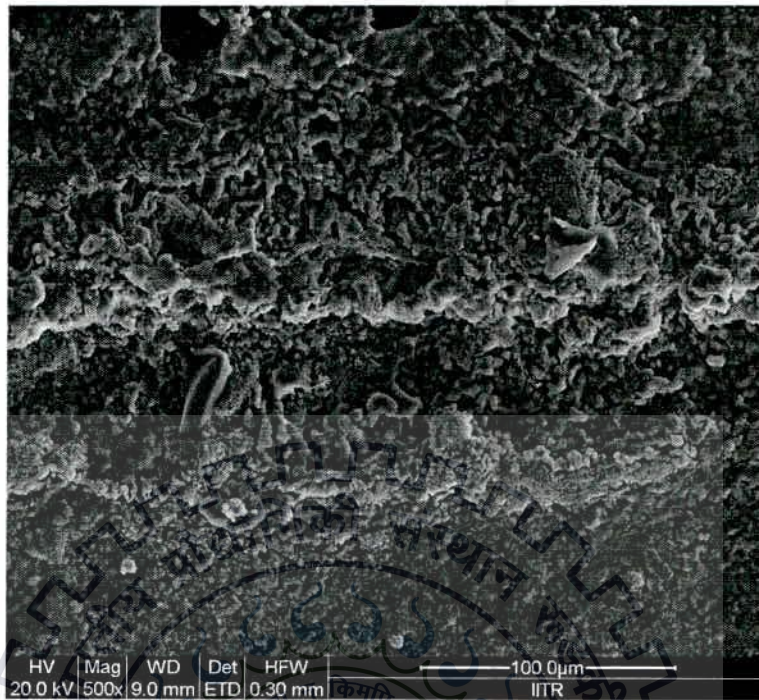


Fig 4.4: FE-SEM image showing the channel region of a device at a magnification of 500x.



Fig 4.5: FE-SEM image showing the channel region of a device at a magnification of 5000x.

4.2 Spectroscopy results

Elements	Weight %	Atoms %
C	6.83	11.17
O	45.81	56.25
Na	7.65	6.54
Mg	1.75	1.41
Al	0.65	0.47
Ca	7.35	3.2
Si	29.96	20.96
Total	100	100

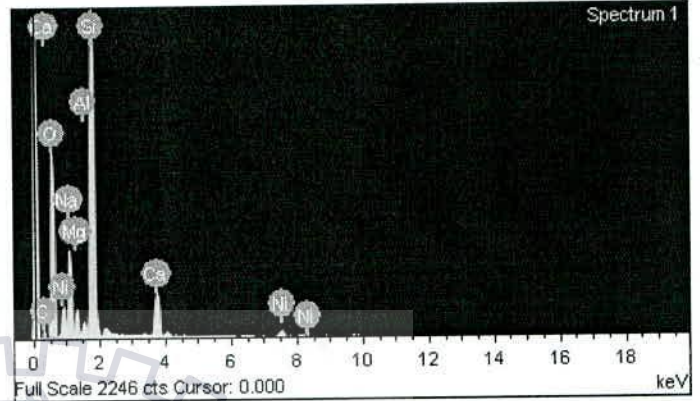


Fig 4.6: Spectrum of channel region before dispersing the solution, Carbon present is due to CaCO_3 in glass.

Table 4.1: Showing the constituents of channel before dispersing the solution.

Elements	Weight %	Atoms %
C	54.22	65.52
O	26.77	24.28
Na	8.95	5.65
S	10.06	4.55
Total	100	100

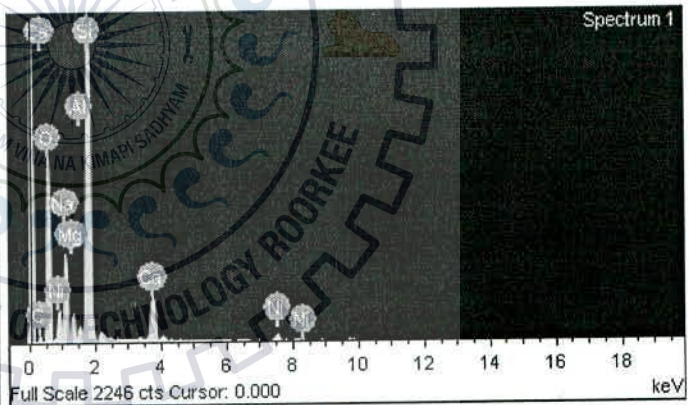


Fig 4.7: Spectrum of channel region after dispersing the solution, Note the increase in carbon content, the sodium & sulfur comes from SDS.

Table 4.2: Showing the constituents of channel after dispersing the solution. The increase in carbon content signifies presence of nanotubes at junction.

Elements	Weight %	Atoms %
C	54.77	65.99
O	27.06	24.47
Na	7.49	4.71
S	10.68	4.82
Total		100

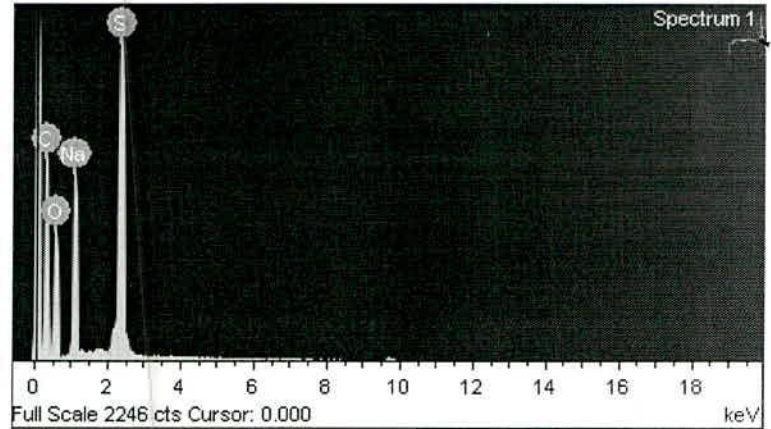


Table 4.3: Showing the constituents of channel after dispersing the solution. The increase in carbon content signifies presence of nanotubes at junction.

Fig 4.8: Spectrum of channel region of another device after dispersing the solution, Note the increase in carbon content, the sodium & sulfur comes from SDS.

Figure 4.6 gives the spectroscopy of channel region before dispersing the CNT solution. Table 4.1 lists the constituent elements as appeared in spectroscopy by their percentage contribution. As the channel region is exposed glass which has not been deposited with metal, high amount of silicon comes from SiO_2 which is the main constituent of glass, remaining Al, Mg, Ca are the salts in glass. Carbon comes from CaCO_3 found in glass.

Figure 4.7 & 4.8 gives the spectroscopy of two different CNT films deposited after centrifuge and decantation. Table 4.2 & 4.3 lists the constituent elements as appeared in spectroscopy by their percentage contribution. Sodium and Sulfur comes from the surfactant sodium dodecyl sulfate. The increased carbon content should come from the CNT as there is no other source of carbon to contribute so high by weight percentage.

4.3 I-V characteristics of the fabricated devices

The fabricated devices will have Schottky barriers, these Schottky diodes will appear as back to back in the equivalent circuit; in between these two diodes there will be a network of CNT connected in random fashion. As these CNTs have different chirality they will have different band structure as well as different Fermi energy; when two semiconducting tubes of different Fermi energies but same band gap meet they will form a homojunction, when two semiconducting tubes of different Fermi energies and different band structure meet they will form a heterojunction, when a metallic and semiconducting tube meet they will form a Schottky barrier.

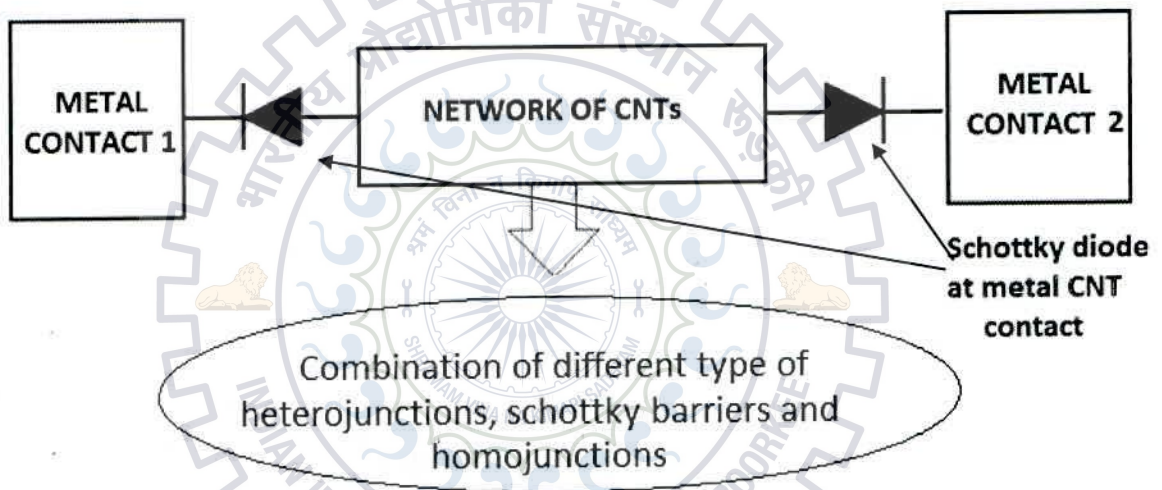


Fig 4.9: Diagram representing the model of the fabricated structure.

So the I-V characteristics of the device become very difficult to predict as the random fashion in which these different junctions are connected cannot be found out plus the other specifications such as the energy barriers of these junctions are unknown; so the I-V characteristics cannot be predicted theoretically. This will also produce device to device level variations as the CNT bundles may be connected in different fashion in different devices.

The Fabricated device showed following I-V Characteristics:

4.3.1 Ni-CNT-Ni Device I-V Characteristics

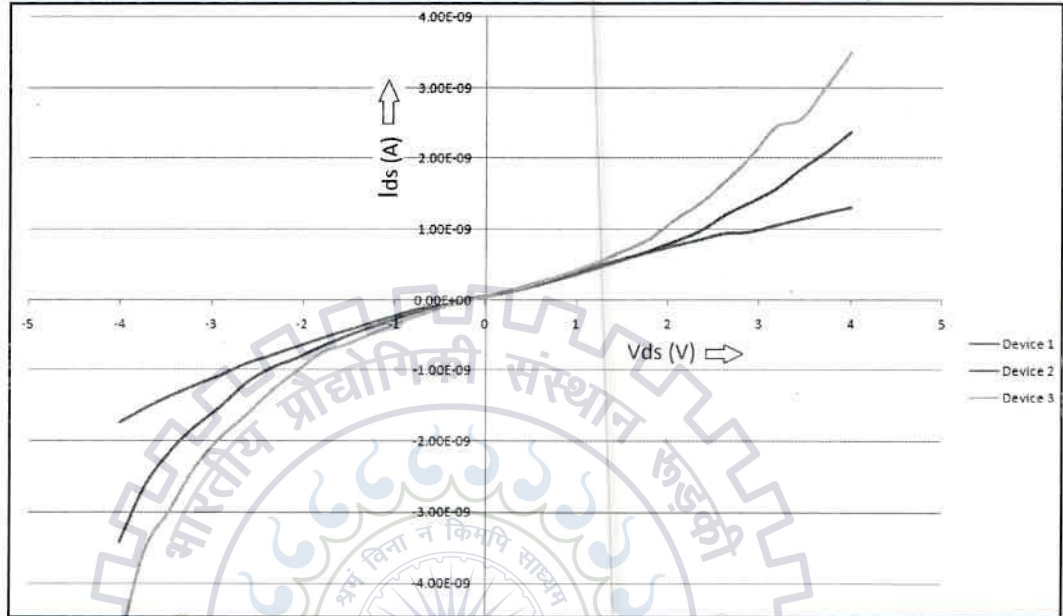


Fig 4.10: I-V Characteristics of Ni-CNT-Ni devices.

Figure 4.10 shows the I-V characteristics of Ni-CNT-Ni contact devices; the voltage across the two electrodes is varied from -4V to 4V, entire interval has been divided into 30 data point intervals and then the current is recorded. The characteristics of these devices show some difference in behavior, few devices always show completely ohmic characteristic and others show different level of non-linearity. The characteristics are not entirely symmetric on both (positive & negative) side of the sweep, though the trend of rise of current with respect to voltage match, but the rise is faster in the negative bias.

4.3.2 Cu-CNT-Cu device I-V Characteristics

Figure 4.11 shows the I-V Characteristics of Cu devices, the I-V characteristics of few Copper contact devices remains completely ohmic on both side of the sweep i.e. completely ohmic devices though showing some difference in the resistance from each other, whereas few devices show some exponential rise in current. The unsymmetrical I-V curves signify difference in the Schottky barrier at the two metal-CNT junctions as already fabricated and tested by Lu et al [14].

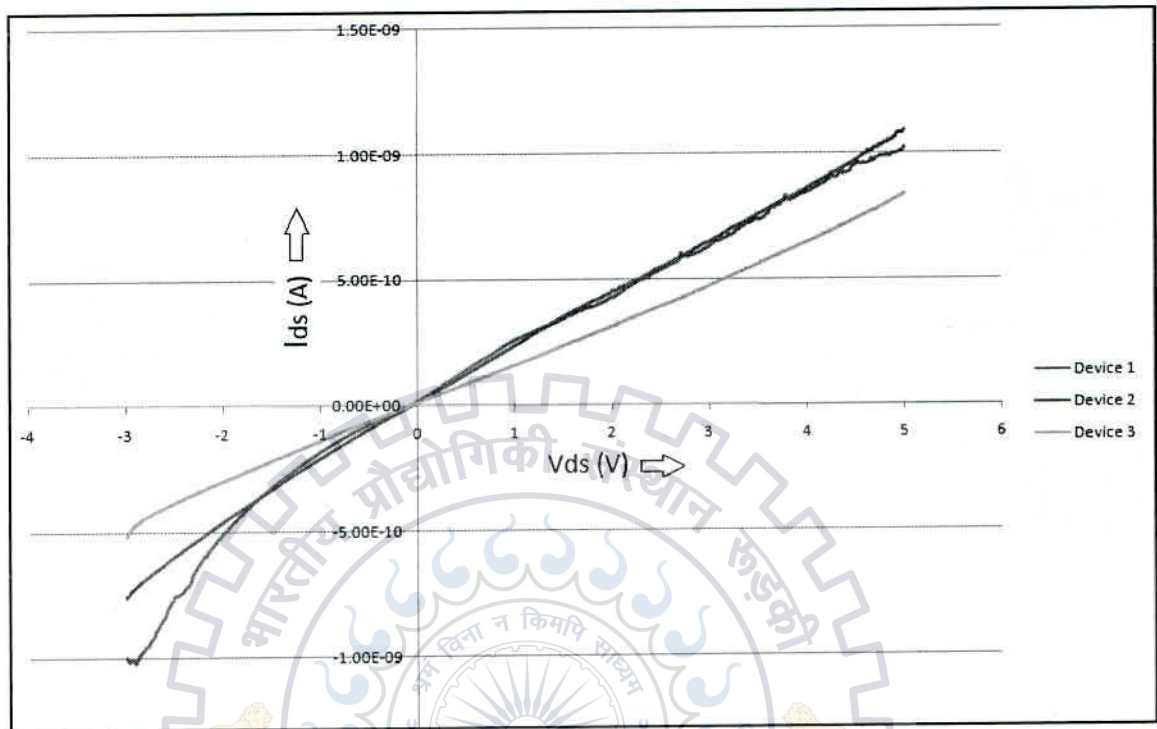


Fig 4.11: I-V Characteristics of Cu-CNT-Cu devices.

4.3.3 Al-CNT-Al device I-V Characteristics

Figure 4.12 shows the I-V characteristics of device fabricated using Aluminum as the contact material shows linear variation of current with voltage and some short term nonlinearities. Device 1 & 3 shows a gradual increase in the conductance as the applied voltage increases whereas device 2 shows a decrease in the conductance with increase in applied voltage at positive side. At the negative applied voltage side the I-V curve of the device remain linear initially showing some change in conductance at the higher voltages but the changes are not similar to that of changes at the positive voltage side.

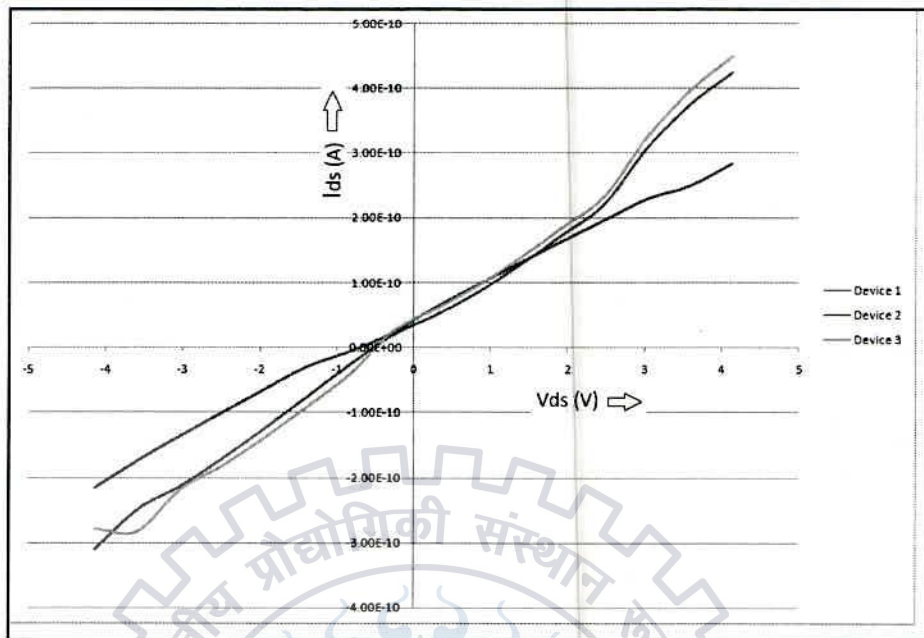


Fig 4.12: I-V Characteristics of Al-CNT-Al devices.

4.3.4 COMPARISON OF I-V CHARACTERISTICS OF Ni, Cu & Al DEVICES.

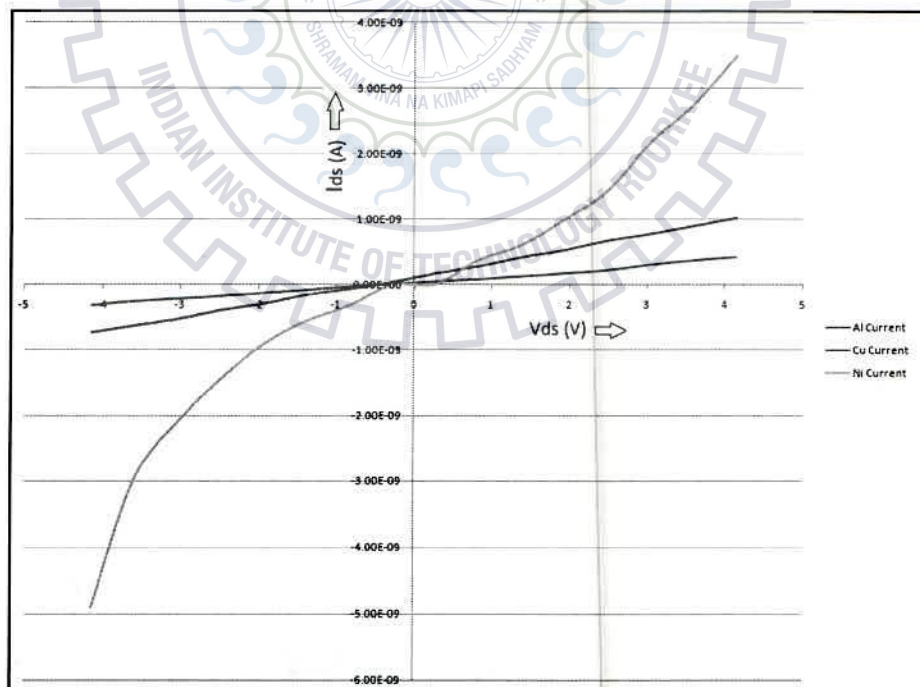


Fig 4.13: Comparison of I-V Characteristics of three different metal-CNT devices.

Figure 4.13 shows the comparison of the three metals (Nickel, Aluminum and Copper) – CNT contact, Nickel has the highest current at any given voltages, while copper has the current higher than that of aluminum; Aluminum shows lowest current. The I-V characteristics of Nickel is exponential in nature and somewhat symmetric, it also resembles to the back to back Schottky diode characteristics. At 4V applied voltage current of Cu device is thrice of that of Al device and the current of Ni device is thrice of that of Cu device.

4.4 Thermionic Emission

Thermionic emission current can be obtained in a device by biasing the device at such a voltage (0.01V in this case) that leads to negligible tunneling in the device across the junction, measure current in the device with increasing temperature. As temperature increases the electron gain extra energy from the heat provided and now can jump over the barrier.

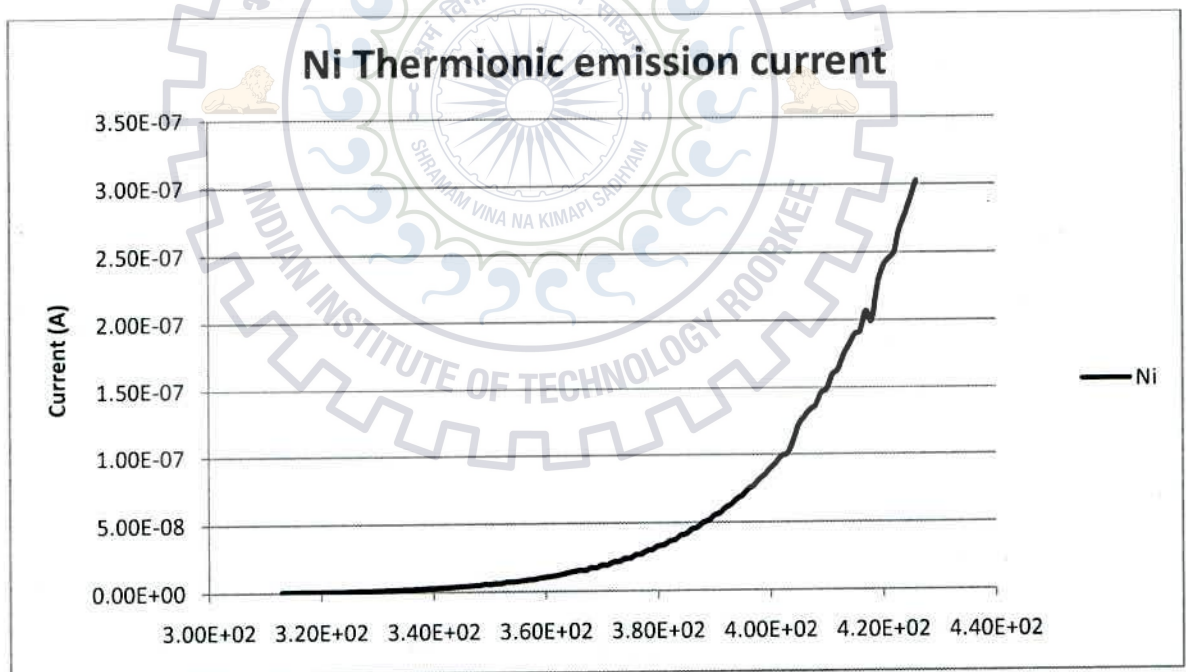


Fig 4.14: Rise in the current through a nickel contact device with temperature at a applied bias of 0.01V.

The thermionic emission current of all three devices shows exponential rise in current with temperature. Figure 4.14 shows the increase in thermionic emission current in nickel device as temperature is varied from 40°C to 150°C, figure 4.15 shows the same plot for copper contacts and figure 4.16 shows for aluminum contacts. The change in current is due to rise in the thermionic emission current as the low applied bias restricts the current from tunneling.

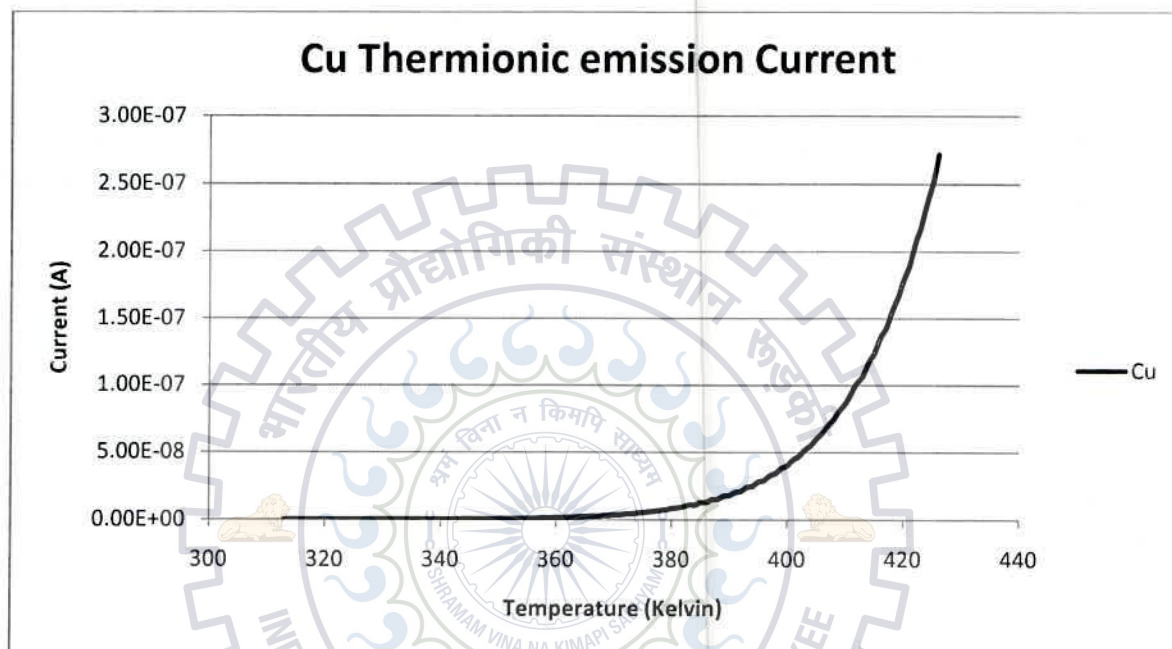


Fig 4.15: Rise in the current through a copper contact device with temperature at a applied bias of 0.01V.

Figure 4.17 shows the comparison of thermionic emission current of three contacts. As we can see from the figure that the exponential raise in current in nickel device starts first, after further heating in copper and at last in aluminum. The nickel current rises slowly as compared to aluminum which rises abruptly with temperature as the exponential part starts.

This clearly establishes that the barrier height at the nickel contact should be minimum and that of the aluminum should be maximum among three with copper having an intermediate.

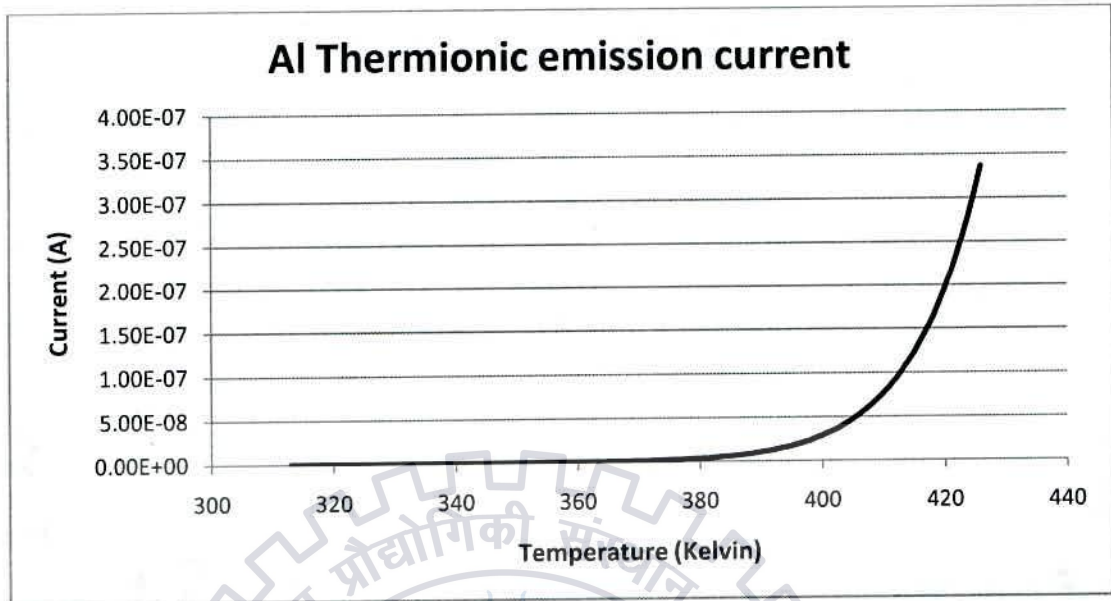


Fig 4.16: Rise in the current through a Aluminum contact device with temperature at a applied bias of 0.01V.

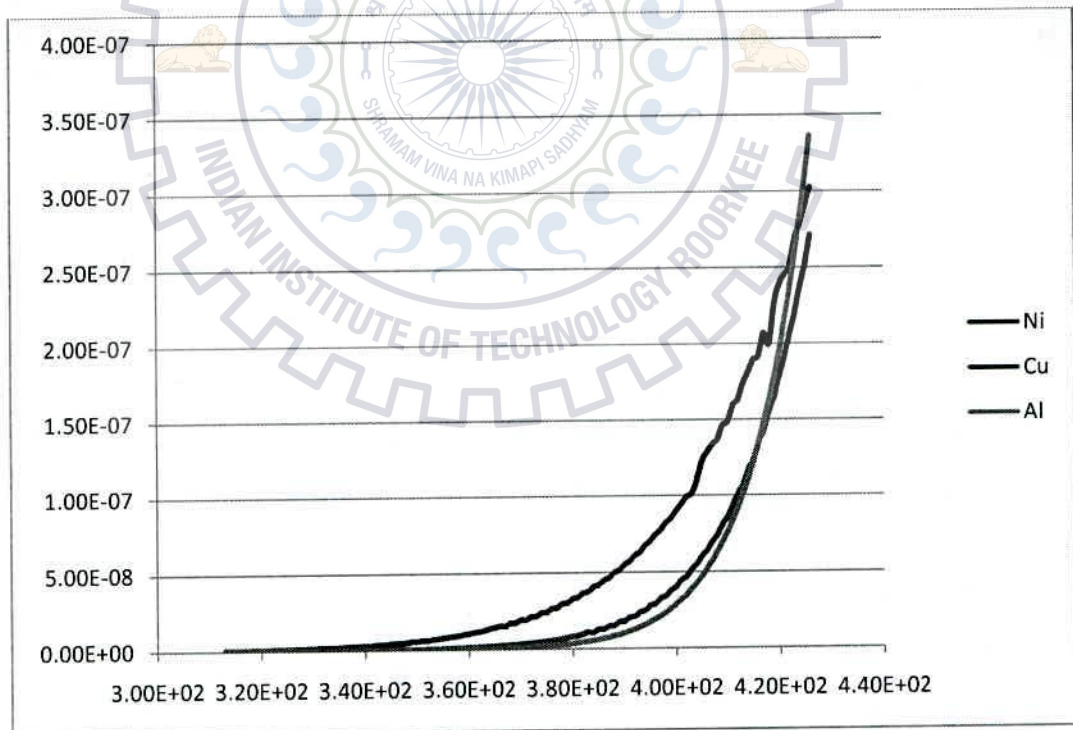


Fig 4.17: Comparison of thermionic current of Ni, Cu and Al devices.

3.2.1 RICHARDSON'S LAW OF THERMIONIC EMISSION

Richardson's law of thermionic emission in solid metals gives the equation for the current density due to thermionic emission as

$$J = AT^2 \exp(-q\phi_B/kT) \quad - 1$$

Taking log on both sides we get

$$\ln(J) = \ln(A) + 2\ln(T) - q\phi_B/kT \quad - 2$$

So plotting $\ln(I/T^2)$ against $1/T$ gives a linear curve for exponential rise, the slope of this curve will be directly proportional to the energy barrier at the metal-CNT contact.

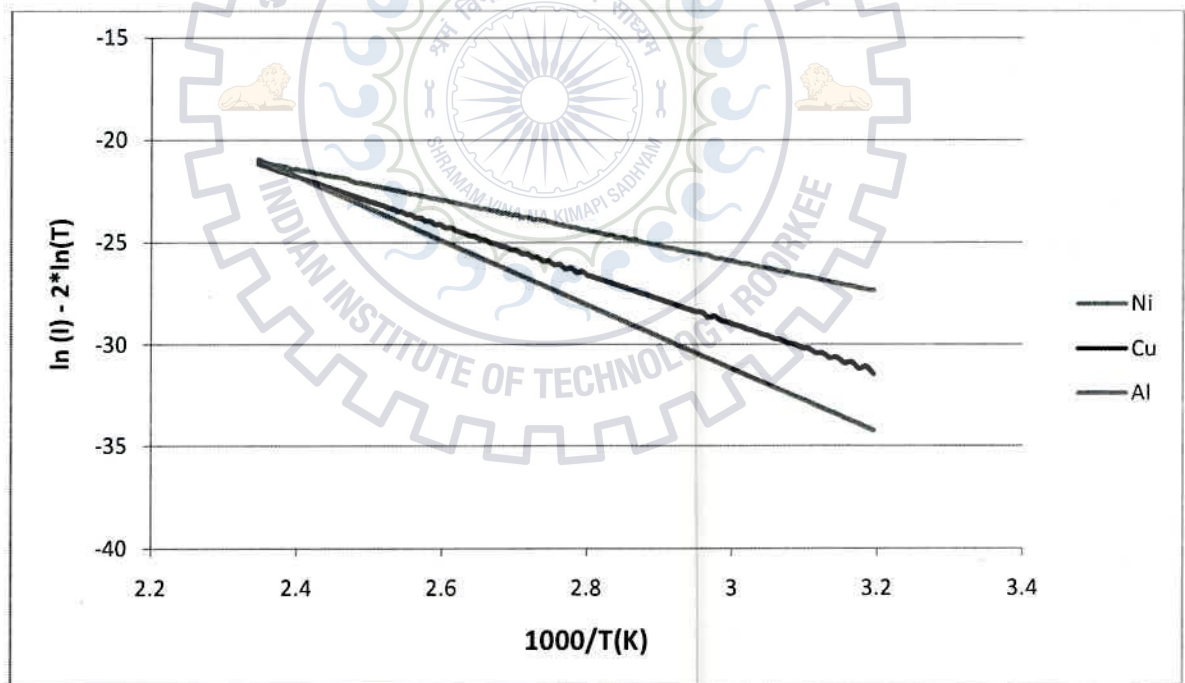


Fig 4.18: Rise in the current through different metal contact device with temperature at an applied bias of 0.01V; the slope of the curve is directly proportional to the energy barrier; the linear curve at log scale represents exponential rise in thermionic emission current.

The slope of the line gives the value “ $q\phi_B/k$ ”, where q is the electronic charge and k is boltzman’s constant. From the slope the value of barrier height can be found which are:

$$\Phi_{\text{Ni-CNT}} = 0.647 \text{ eV}$$

$$\Phi_{\text{Cu-CNT}} = 1.055 \text{ eV}$$

$$\Phi_{\text{Al-CNT}} = 1.363 \text{ eV}$$

$$\Phi_{\text{Al-CNT}} > \Phi_{\text{Cu-CNT}} > \Phi_{\text{Ni-CNT}}$$

The energy barrier at the metal-CNT contact is highest in the case of Aluminum then Copper and then the least in the case of Nickel as demonstrated by the comparison of I-V characteristics in figure 4.13 and in comparison of thermionic emission current in figure 4.17.

We know the work function of these metals [26] which are

$$\Phi_{\text{Al}} = 4.08 \text{ eV}$$

$$\Phi_{\text{Cu}} = 4.7 \text{ eV}$$

$$\Phi_{\text{Ni}} = 5.01 \text{ eV}$$

The barrier height of the contact can be evaluated if by

$$\Phi_{\text{M-CNT}} = \Phi_{\text{CNT}} - \Phi_{\text{M}}$$

Where,

$\Phi_{\text{M-CNT}}$ = barrier height of the contact,

Φ_{CNT} = Work function of CNT

Φ_{M} = Work function of the metal

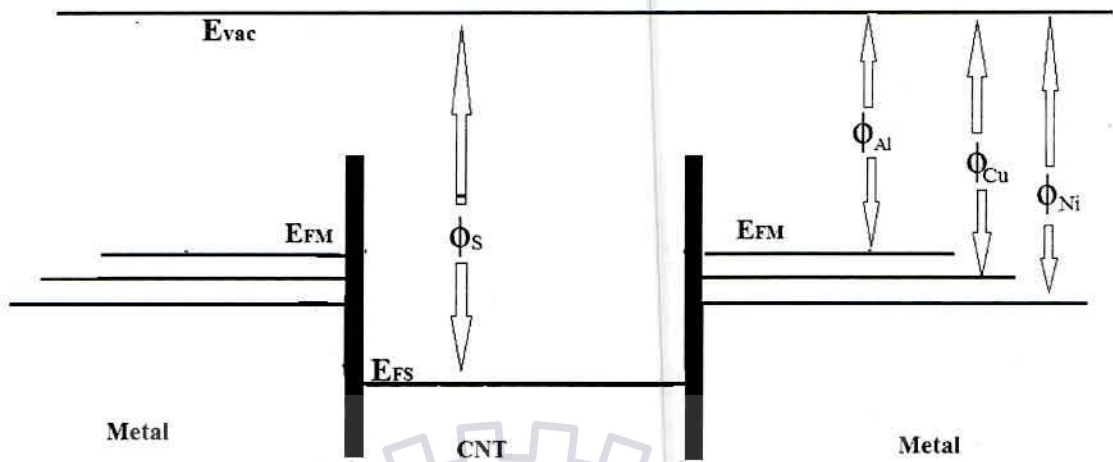
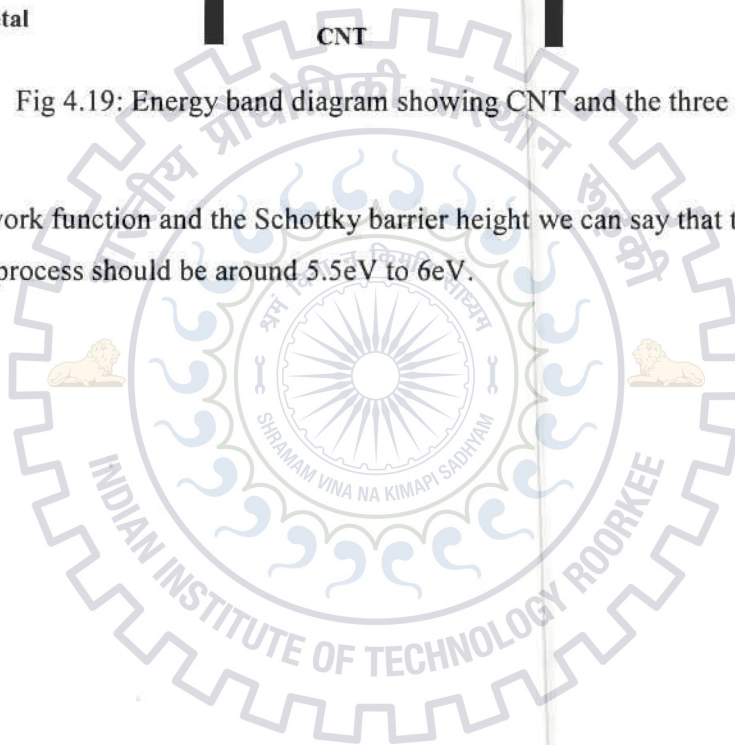


Fig 4.19: Energy band diagram showing CNT and the three metals.

So from the work function and the Schottky barrier height we can say that the Fermi level of the CNTs in this process should be around 5.5eV to 6eV.



4.5 Effect of Gas on the Devices

4.5.1 CARBON DIOXIDE GAS

The Device is tested for the IV characteristics first and a suitable bias point is taken; the device is biased at that particular voltage which is 1.5V in this particular case. First of all reading is taken for 45 seconds before the application of gas; then gas is applied at the flow rate of 1ltr/min for 45 seconds. The current was around 1nA before the application of gas; we were measuring current every quarter of second i.e. 4 data points per second, as we applied gas within fractions of second current dropped 20 times to 0.05nA, this change happened within 0.25seconds and within 15 seconds current dropped 125 times to 0.008nA. As the gas application is stopped the current slowly started to recover as shown by the table below:

Time after application of Gas (sec)	Conductance (nS)	Percentage of Initial %	Relative change from the previous
0	0.00586	0.88%	-
100	0.02067	3%	3.5
200	0.0317	4%	1.53
300	0.0520	5%	1.09
400	0.3467	17%	3.27
500	0.14	21%	1.23

Table 4.4: Showing the change in conductance of the device with respect to time after application of carbon dioxide

The table 4.4 suggests that current is recovering by desorption of Carbon dioxide gas, the desorption process is endothermic in nature because the already captured molecule require some energy from the ambient to set free, so increasing the temperature will assist in the process and the natural rate of desorption will slow down as the no. of molecule adsorbed decreases. So we increased the temperature of the device from room temperature to 125°C, this accelerated the process of desorption and within 3 minutes the current increased from 0.25nA to 6nA a 24 times increase. The current overshoots the initial value, after that current changes value and stabilize to the initial only after 2 hours.

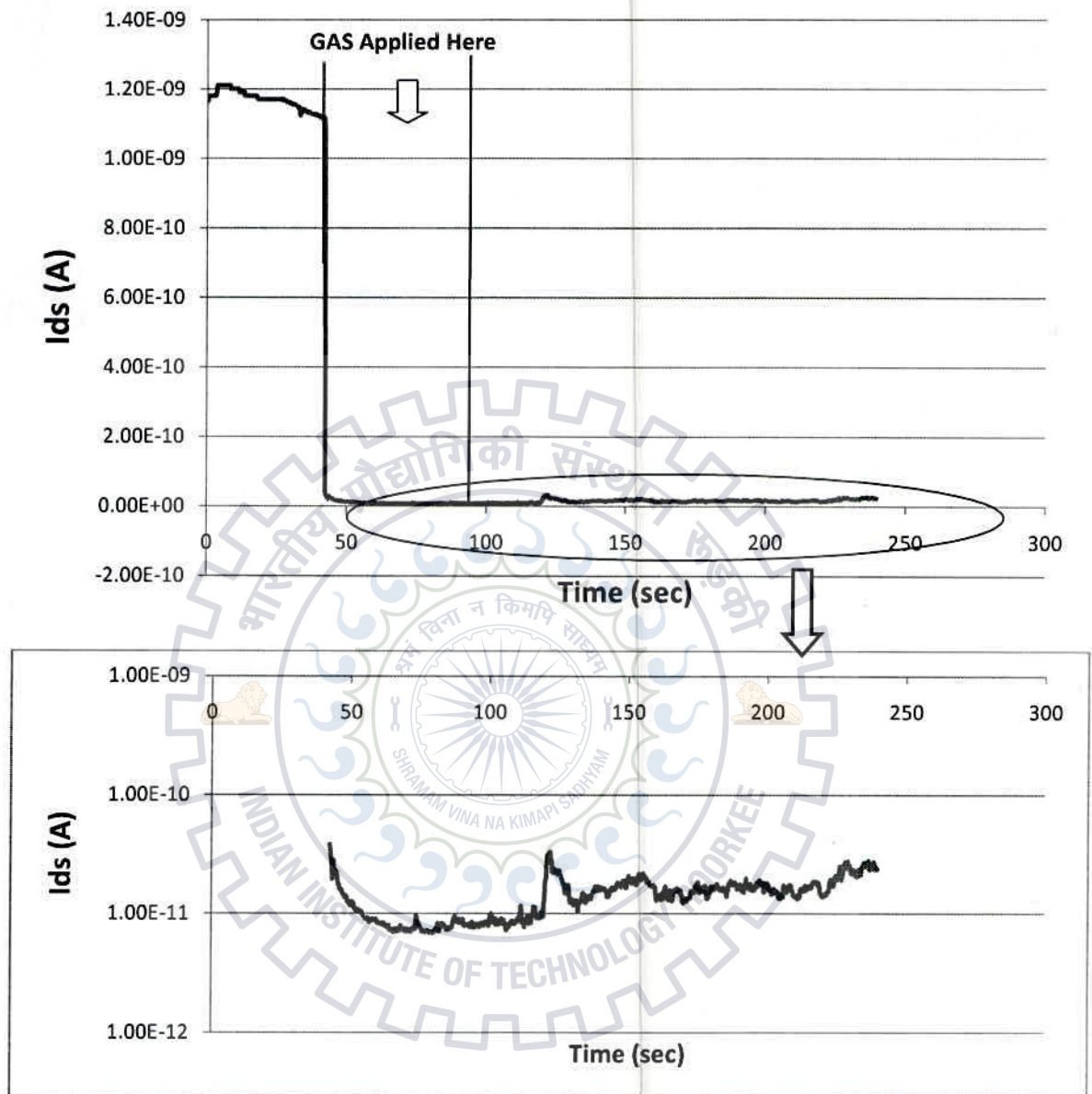


Fig 4.20: Plot Showing the Effect of Application of Carbon Dioxide gas on the device.

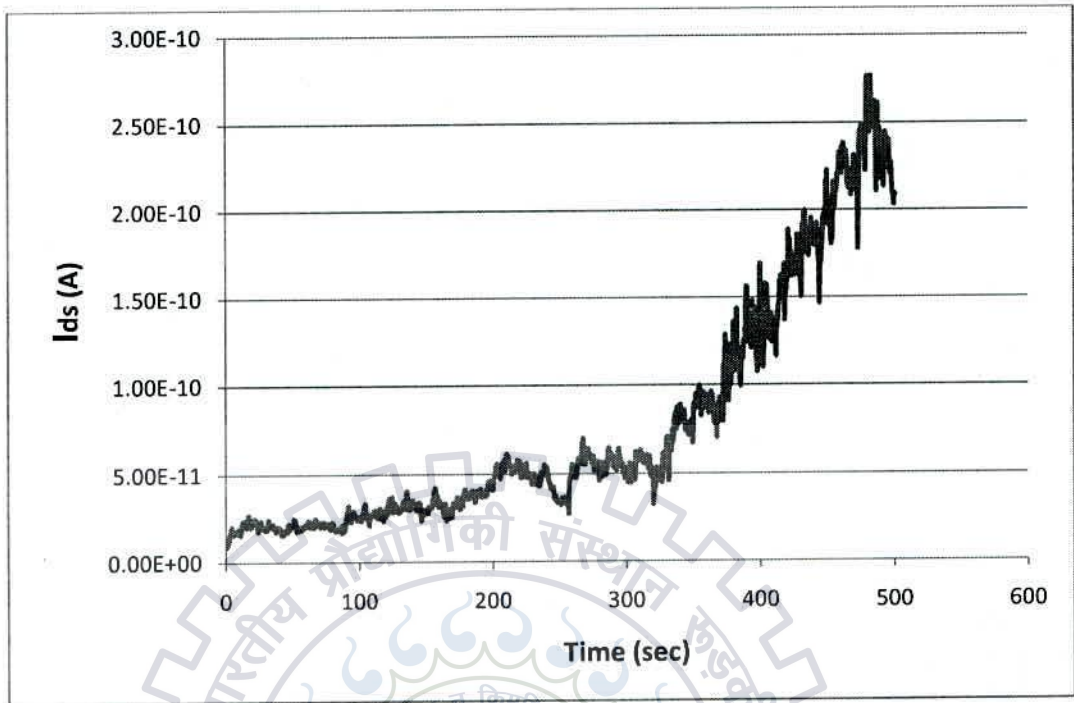


Fig 4.21: Plot showing a 12 minutes sweep just after the application of Carbon Dioxide gas on the device.

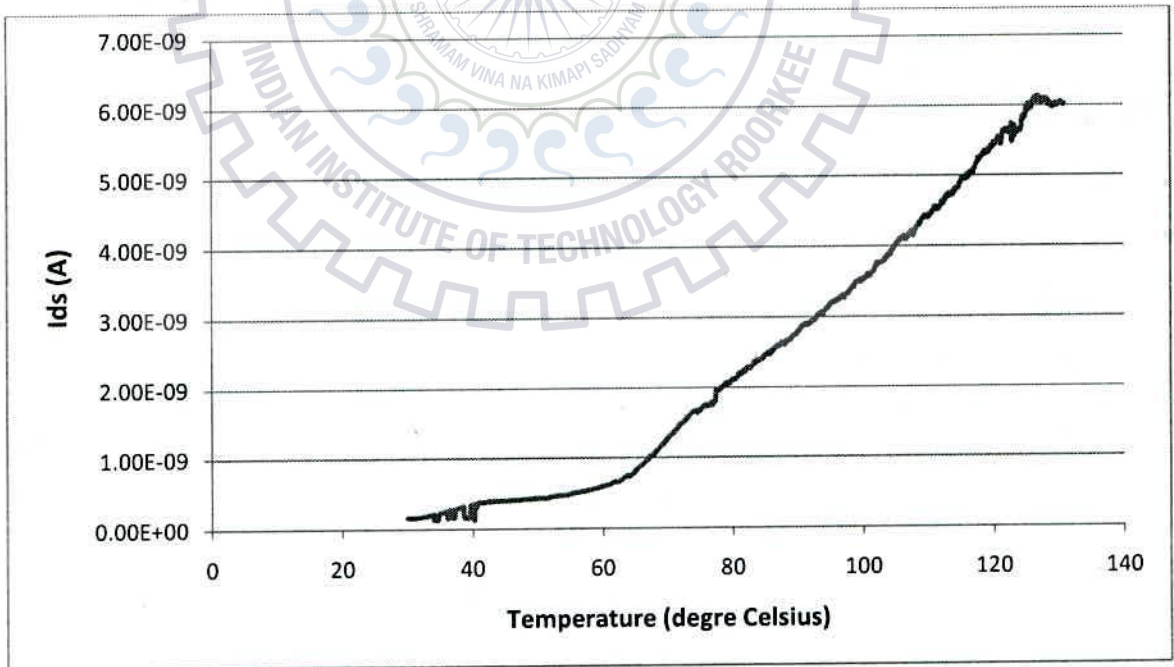


Fig 4.22: Increase in temperature leads to desorption of the adsorbed gas.

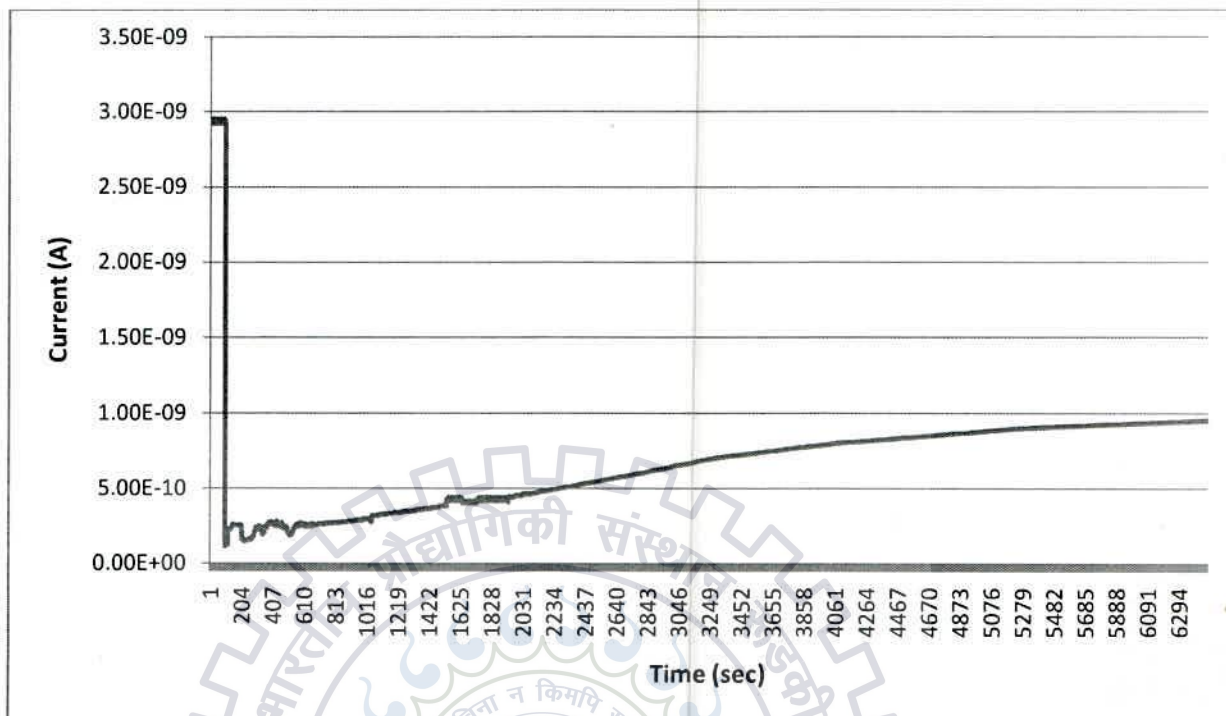


Fig 4.23: Plot Showing the Effect of Application of Carbon Dioxide gas on the device. Here the recovery occurs without providing heat. Initially the recovery is fast then it slows down and saturates.

DEVICE	RESPONSE TIME (sec)	RECOVERY TIME (sec)
Ni- CNT- Ni	0.5	2 hours
Al- CNT-Al	0.75	1 hour, subjecting to heat after 50 minutes.

Table 4.5: Table showing the response time and recovery time of Carbon Dioxide on different metal- CNT devices.

3.4.2 NITROGEN GAS

Nitrogen gas with a triple bond is very stable and inert in nature and doesn't interact with a lot of species; when we performed experiments on nitrogen it didn't produce a consistent and repeatable result

Figure 3.12 shows a plot where initially before application of N_2 gas the Al-CNT device current was around 0.25nA after application of gas current reduces drastically but recover within few seconds and then again decreases to 5% of that of initial value, as the application of gas ceases the current again recover to initial value within few seconds.

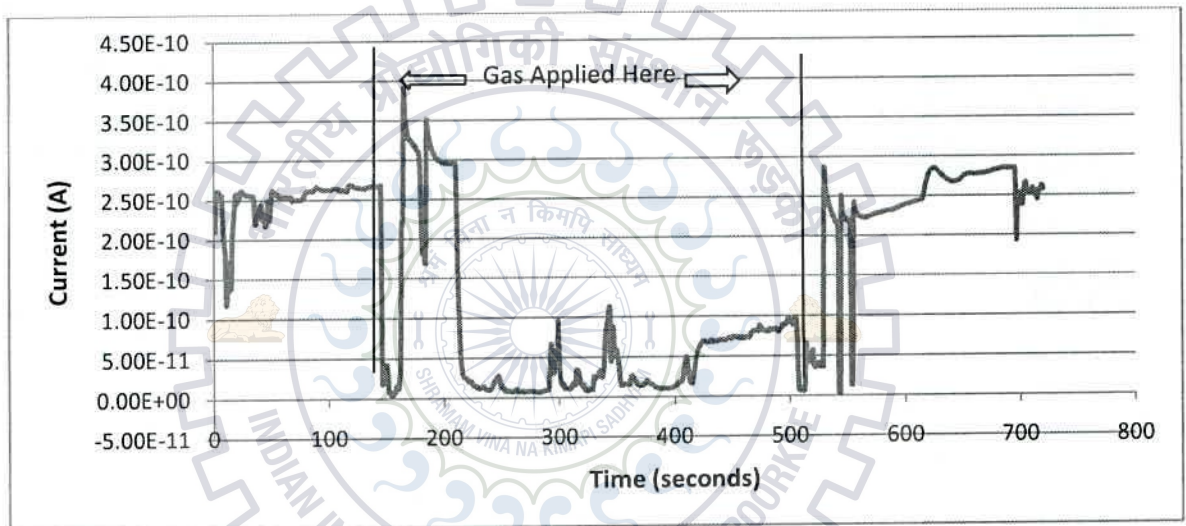


Fig 4.24: Plot showing the effect of application of N_2 gas on Al-CNT device; the current decreases 20 times in presence of gas and recover very fast to initial value as the gas ceases.

Whereas in another device as shown in figure 3.13 initially current was very low in the order of few pA, on application of N_2 gas the current rises as much as to the 70 times of the initial value but as the gas application is stopped the current recover back to its initial value showing no after effect of presence of gas; figure 3.13 demonstrates this fact.

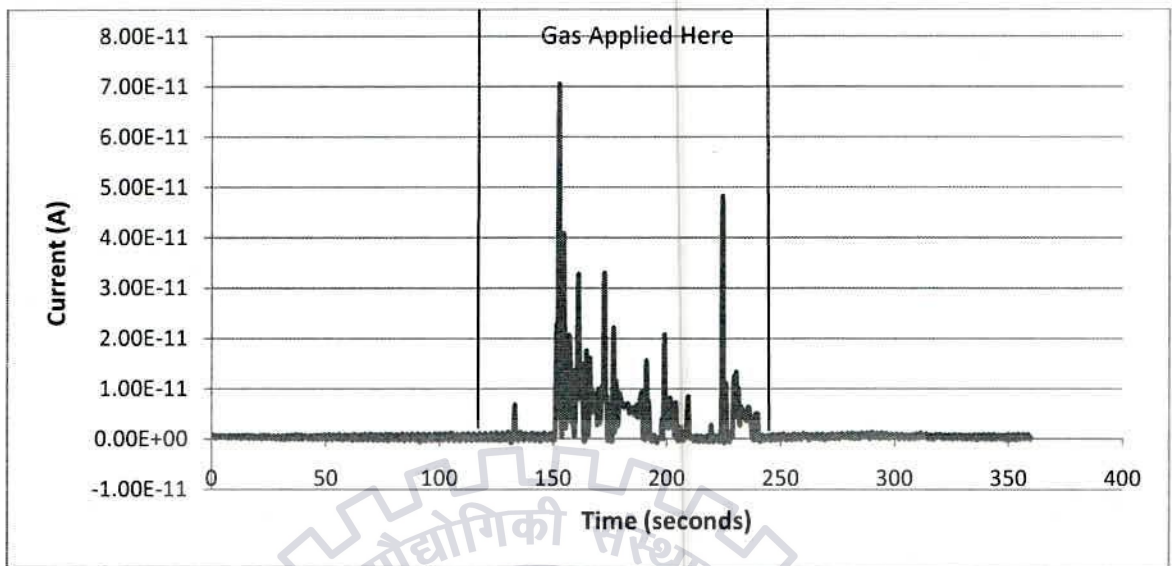


Fig 4.25: Plot showing the effect of application of N_2 gas on Al-CNT device; the current decreases 20 times in presence of gas and recover very fast to initial value as the gas seizes.

In another experiment the current decreases every time in the presence of gas but this time the recovery time is longer (about 80 seconds), figure 3.14 demonstrates this fact.

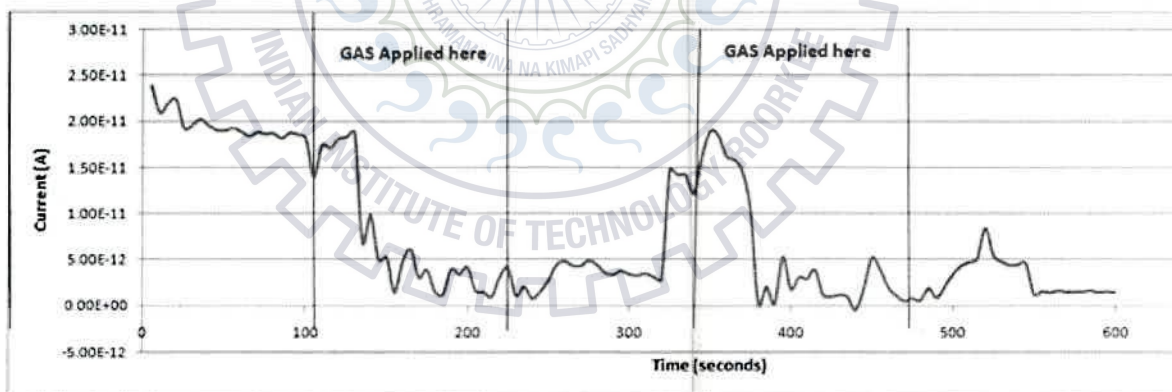


Fig 4.26: plot showing the effect of application of N_2 gas on Al-CNT device; the current decreases every time in the presence of gas.

So, nitrogen generally decreases the current but the recovery time varies from few seconds to 100 seconds in different cases and some time it increases the current also.

DEVICE	RESPONSE TIME (sec)	RECOVERY TIME (sec)
Al- CNT-Al	30	139
Al- CNT- Al	85	48
Al- CNT-Al	102	112

Table 4.5: Table showing the response time and recovery time of Nitrogen on Al- CNT devices.

3.4.3 A MIXTURE of CH_4+CO_2 IN THE 1:1 PROPORTION.

We applied a mixture of Methane and Carbon Dioxide in a Al-CNT device the current which initially was around 30 pA increases around 30 to 50 times after few seconds of application of gas. As we stopped applying gas the current took a steady state value of 0.55nA which was around 20 times of that of initial value.

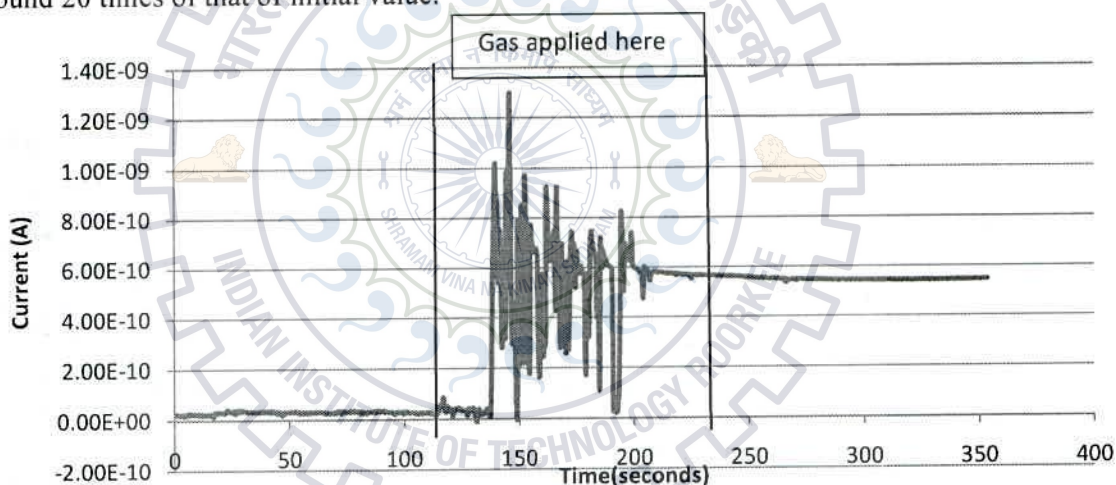


Fig 4.27: Plot showing the effect of application of CH_4+CO_2 gas on Al-CNT device; the current increases on application of gas and then maintains a steady state value even after the gas which is 20 times that of the initial value of current.

The effect of the adsorbed gas doesn't remains even after half an hour of application of gas as shown by figure 3.16.

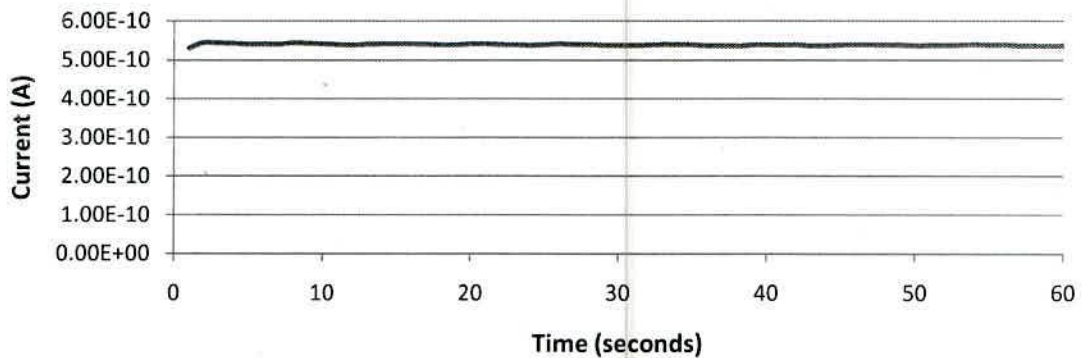


Fig 4.28 :Plot showing the after effect of application of CH_4+CO_2 gas on Al-CNT device; the current maintains its steady state value as achieved just after the gas even half an hour later.

Heating the device at 100°C and then letting the gas around the device to disperse led the device to regain its initial value of current.

To check for sensitivity of this gas mixture we applied a small pinch of this mixture to a device the current rose up 100 times (figure 3.17) that of the initial value and maintained that value showing a very small rate of desorption.

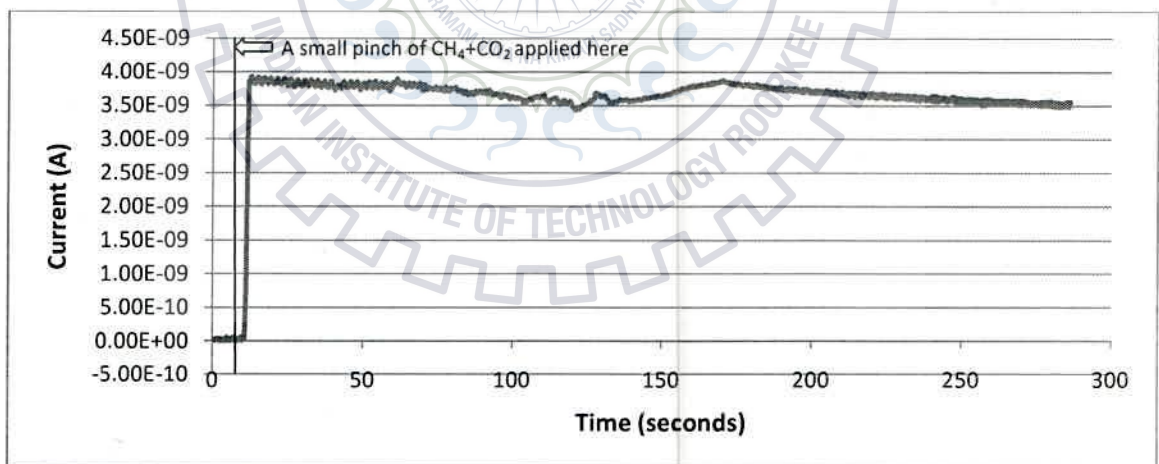


Fig 4.29: plot showing the effect of application of very small amount of CH_4+CO_2 gas on Al-CNT device; the current rose by 100 times in a second and maintains this high value.

To cross check, we applied nitrogen just after the above case, the current shows some variations, rising and falling but finally current settled down to about 0.3nA around 10% of that of the initial value.

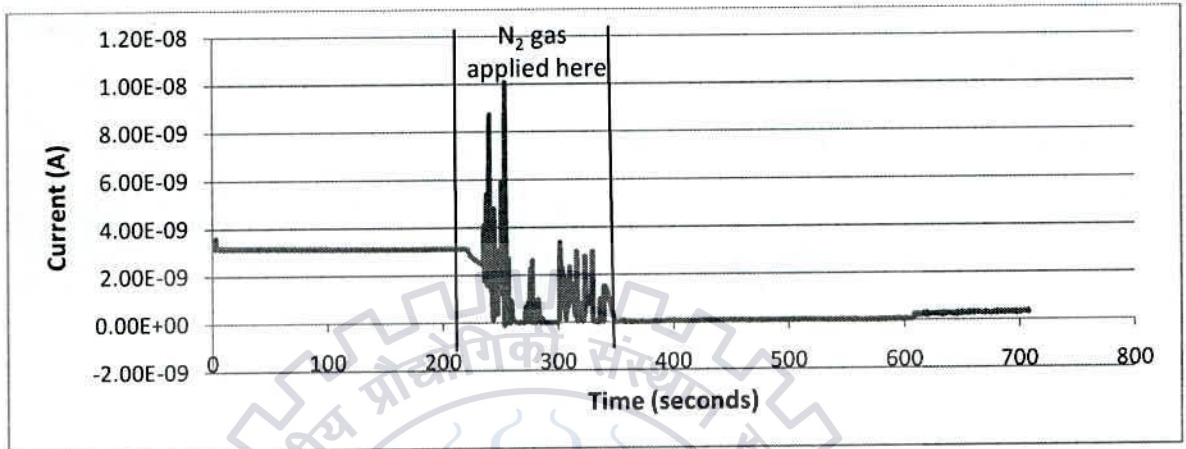


Fig 4.30: Plot showing the effect of application of Nitrogen after the current in the device is in steady state after application of very small amount of $\text{CH}_4 + \text{CO}_2$ gas on Al-CNT device; the current decreases by 10 times in few second and maintains this value.

5. Conclusion

- Two terminal device using CNT as channel and three different metals (Nickel, Copper and Aluminum) as contact were fabricated and their I-V characteristics were obtained.
- Nickel contact devices showed maximum conductance and Aluminum contact devices showed minimum conductance, copper devices were intermediate of the two.
- Difference in conductance of the devices was due to difference in the Schottky barrier at the metal-nanotube contacts as demonstrated by thermionic emission results of the three devices, the nickel contact shown the Schottky barrier of 0.647 eV, copper device gave the barrier height as 1.055 eV and Aluminum device gave 1.36 eV.
- The work function of different metal and the Schottky barrier establishes that the CNT must be p-type with work function value around 6 eV.
- Application of Carbon Dioxide Gas decreases the conductance of the device by as much as 100 times within fractions of seconds and desorbs very slowly, only after heating the device up to 100°C the gas desorbs and the initial conductance can be restored.
- Application of Nitrogen generally decreases the conductance but sometimes it has increased the conductance too, the recovery time also varies from few seconds to 100's of seconds.
- Application of a mixture of Methane and Carbon dioxide increases the conductance by large values (in the order of 300 to 500 times) with a response time of fractions of seconds and desorbs very slowly; it maintained the value achieved after exposure up to hours and could be restored to initial value only by heating the device up to 100°C.

References

1. S. Iijima, "Helical Microtubules of graphitic carbon," *Nature*, vol. 354, pp 56-58, 1991.
2. A. Javey, J. Kong, "Band Structure and Electron Transport Physics of One-Dimensional SWNTs," in *Carbon Nanotube Electronics*, 2nd Edition, Springer-Verlag, 2009.
3. Meyyappan M, "Carbon Nanotubes: Science and Applications". Boca Raton CRC Press (2005).
4. J Kong, H T Soh, A M Cassell, C F Quate and H J Dai, Synthesis of individual single-walled carbon-nanotubes on patterned silicon wafers, *Nature*, vol. 395, pp. 878-881, 1998.
5. Y P Sun, Fu K, Lin Y and Huanq W, Functionalized carbon nanotubes properties and applications, *Acc Chem Res*. 35(12), pp. 1096-1104, 2002.
6. Niraj Sinha, Jiazhi Ma and John T. W. Yeow, Carbon Nanotube based sensors. *Jr. Nanoscience and Nanotech*, vol. 6, pp. 573-590, 2006.
7. J. Zhao, A. Buldum, J. Han, and J. P. Lu, "Gas molecule adsorption in carbon nanotubes and nanotube bundles", *Nanotechnology*, vol. 13, pp 195-200, 2002.
8. J. Kong, N. R. Franklin, C. Zhou, M. G. Chapline, S. Peng, K. Cho, and H. Dai, "Nanotube Molecular Wires as Chemical Sensors", *Science*, vol. 287, pp 622-625, 2000.
9. J. Suehiro, H. Imakiire, S. Hidaka, W. Ding, G. Zhou, K. Imasaka, and M. Hara, "Schottky-type response of carbon nanotube NO₂ gas sensor fabricated onto aluminum electrodes by dielectrophoresis" *Sensors and Actuators B*, vol. 114, pp 943-949, 2006.
10. C.Y. Lee, S. Baik, J. Zhang, R. I. Masel and M.S. Strano, "Charge Transfer from Metallic Single-Walled Carbon Nanotube Sensor Arrays," *J. Phys. Chem. B*, vol. 110(23), pp 11055-11061, 2006.
11. E. H. Rhoderick, R. H. Williams, "Metal-semiconductor contacts", 2nd Edition, Clarendon Press, 1988.
12. A.M. Cowley and S.M. Sze, "Surface States and Barrier Height of Metal-Semiconductor Systems", *J. Appl. Phys.*, vol 32, pp 3212-3220, 1965.
13. V Heine, "Theory of Surface States", *Phys. Rev.*, vol 138 (6A), 1965.
14. C Lu, Lei Au, H Zhang et al, "Schottky diodes from asymmetric metal-nanotubes", *App. Phys. Let.*, vol. 88, 133501-3, 2006.

15. H.-S. Philip Wong, Deji Akinwande, "Carbon Nanotube Field effect Transistor" in Carbon Nanotube and Graphene Device Physics, 1st ed., Cambridge Univ. press, 2011.
16. A. Javey, J. Guo, Q. Wang, M. Lundstorm, and H. Dai, "Ballistic carbon nanotube field-effect transistors", Nature, vol. 424, pp 654-657, 2003.
17. D.Dai, Y. Ismail, Wei Wang, H. Ladak, "Powder-based fabrication techniques for single-wall carbon nanotube circuits", IEEE Circuits & Systems, vol. 3, pp. 701-704, 2004.
18. O'connell, Michael J., et al. "Band gap fluorescence from individual single-walled carbon nanotubes", Science, vol. 297, 593-596, 2002.
19. Shim, Hyung Cheoul, et al. "Purification of carbon nanotubes through an electric field near the arranged microelectrodes", Nanotechnology, vol. 18, pp no. 115602-6, 2007.
20. Chen, X. Q., et al. "Aligning single-wall carbon nanotubes with an alternating-current electric field", Applied physics letters, vol. 78.23, pp no. 3714-3716, 2001.
21. Jiang, Linqin, Lian Gao, and Jing Sun. "Production of aqueous colloidal dispersions of carbon nanotubes", Journal of Colloid and Interface Science, vol. 260.1, pp no. 89-94, 2003.
22. Zhang, Ting, et al. "Recent progress in carbon nanotube-based gas sensors."Nanotechnology, vol. 19.33, pp no. 332001-4, 2008.
23. Zhang, Y., and S. Iijima. "Elastic response of carbon nanotube bundles to visible light" Physical review letters, vol. 82.17, pp no. 3472-3475, 1999.
24. Hertel, Tobias, Richard Martel, and Phaedon Avouris. "Manipulation of individual carbon nanotubes and their interaction with surfaces", The Journal of Physical Chemistry B vol. 102.6 , pp no. 910-915, 1998.
- 25.K. Yamamoto, S. Akita, Y. Nakayama, "Orientation and purification of carbon nanotubes usingac electrophoresis", J. Phys. Appl. Phys., vol. D31, pp. L34-L36, 1998.
26. <http://www.hyperphysics.phy-astr.gsu.edu/hbase/tables/photoelec.html>.

Appendix A: Technical Specifications of Multiwalled Carbon Nanotubes

Purity: > 95%,

Outside Diameter: 10-20nm, Inside Diameter: 5-10 nm,

Length: 0.5-200 μm , SSA: 40-600 m^2/g ,

Bulk density: 0.06 g/cm^3 , True density: $\sim 2.1 \text{ g}/\text{cm}^3$,

Young's modulus (Gpa): ~ 1200 , Tensile strength (Gpa): ~ 150 ,

Thermal conduct (W/m.k): ~ 1200 ,

Viscosity: zero, Color: black

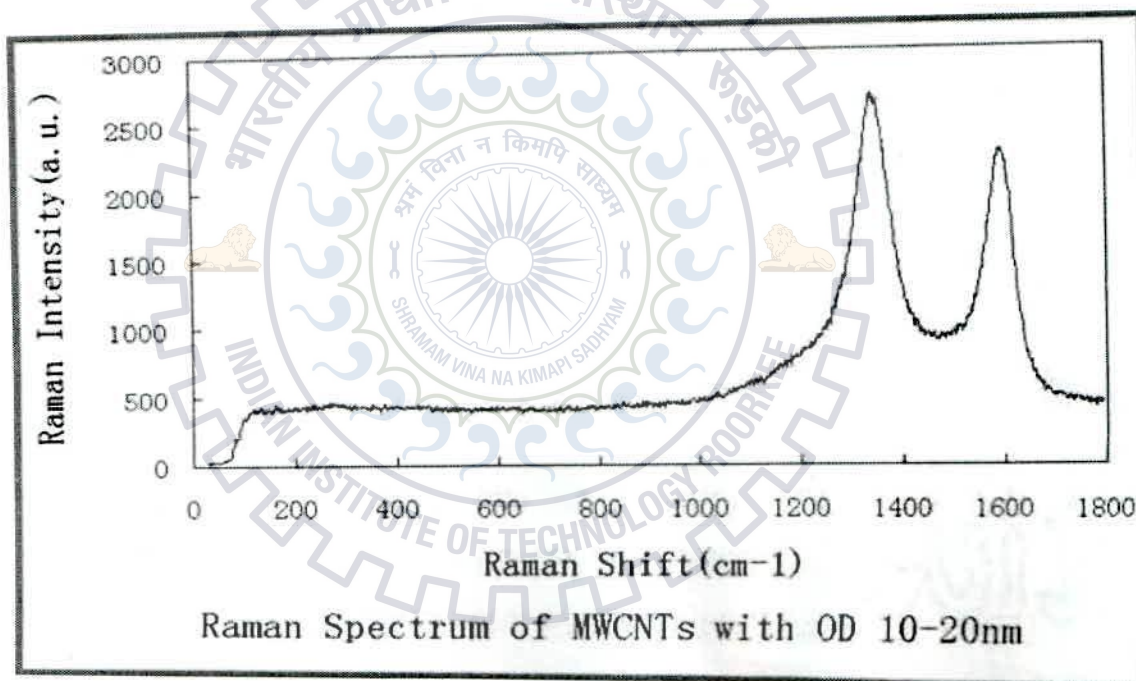


Fig A.1: Raman Spectra of MWNT used in the Fabrication.

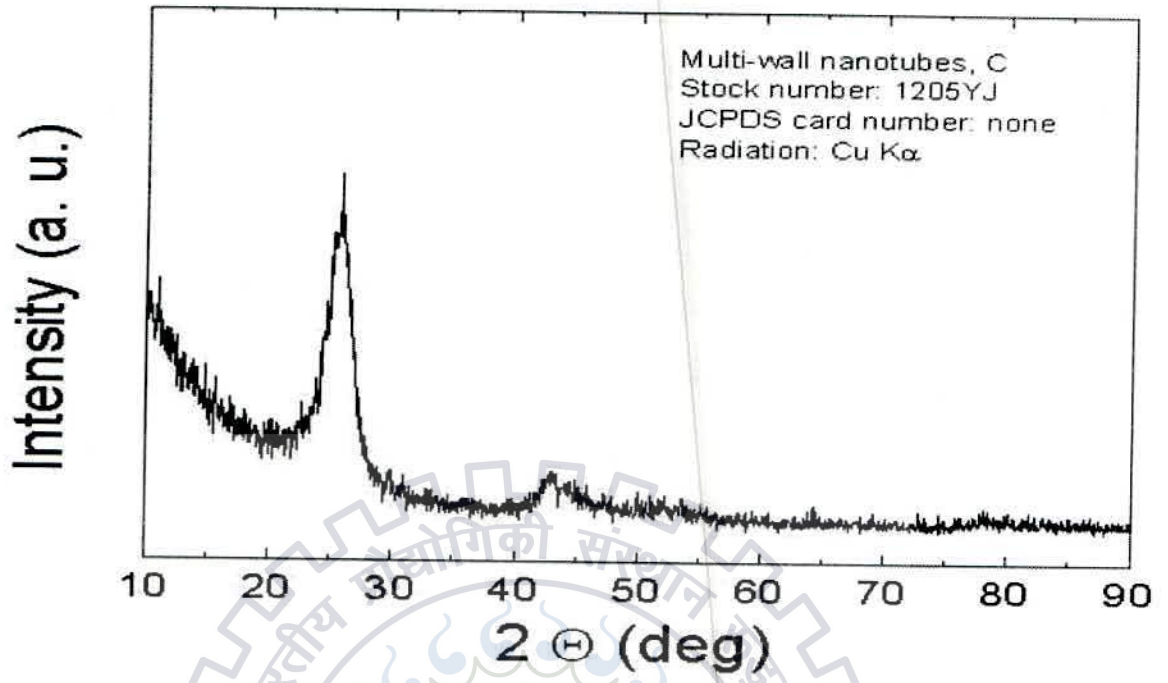


Fig A.2 : X ray diffraction pattern of MWNT used in the Fabrication.